

AUTOMOTIVE EXHAUST EMISSION CONTROL: OXIDATION OF CO ON PEROVSKITE CATALYSTS

A DISSERTATION

*Submitted in partial fulfillment of the
requirements for the award of the degree*

of

MASTER OF TECHNOLOGY

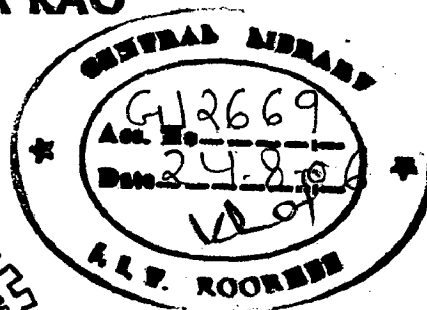
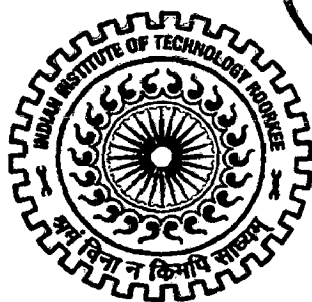
in

CHEMICAL ENGINEERING

(With Specialization in Industrial Pollution Abatement)

By

DEMULA RMA RAO



**DEPARTMENT OF CHEMICAL ENGINEERING
INDIAN INSTITUTE OF TECHNOLOGY ROORKEE
ROORKEE - 247 667 (INDIA)
JUNE, 2006**

CANDIDATE'S DECLARATION

I here by declare that the work, which is being presented in the dissertation work, entitled "**Automotive Exhaust Emission Control: Oxidation of CO on Perovskite Catalysts**", submitted in partial fulfillment of the requirements for the award of **Master of Technology in Chemical Engineering** with the specialization in **Industrial Pollution Abatement, Indian Institute of Technology Roorkee, Roorkee** is an authentic record of my own work carried out during the period from July 2005 to June 2006 under the guidance of **Dr.Shri Chand**, Professor & head, Chemical Engineering Department ,Indian Institute of Technology Roorkee, Roorkee.

The matter embodied in this project work has not been submitted for the award of any other degree.

Date: 28.06.06

Place: Roorkee


(VEMULA RAMA RAO)

CERTIFICATE

This is to certify that the above statement made by the candidate is correct to the best of my knowledge and belief.



Dr. Shri Chand
Professor & Head
Department of Chemical Engineering,
Indian Institute of Technology Roorkee,
Roorkee-247667, India.

ACKNOWLEDGEMENT

I take the opportunity to pay my regards and deep sense of gratitude to my guide **Dr.Shri Chand**, Professor & Head, Department of Chemical Engineering, Indian Institute of Technology Roorkee, Roorkee, for his valuable guidance, keen co-operation, constant inspiration and cheerful encouragement through out the work.

I am thankful to **Dr.I.D.Mall**, Professor, Department of Chemical Engineering, Indian Institute of Technology Roorkee, Roorkee, for providing me all the possible support.

I am also thankful to **Mr.Ayodhya Prasad**, **Mr.Satpal**, **Mr.Harbans Singh** of the Department of Chemical Engineering, for their kind and timely co-operation rendered while working in their laboratories.

I am deeply indebted to Mr.Anil Chandrakar, Mr.Mathur, Mr.K.Upender reddy, Research Scholars, Department of Chemical Engineering, IIT Roorkee, Roorkee, for their kind co-operation during the experimentation.

Special thanks are also due to my friends Venu Gopala Reddy, Sridharan, Vivek Kumar, Vamsi Krishna, Giri Prasad and Ravi Prakash for their constant support and encouragement to finish this work.

I am happy to express my gratitude to my family whose love and blessings made this possible.

Finally, I would like to thank all those who have helped me during this work.

V. Ramanao
(Vemula Rama Rao)

ABSTRACT

Air pollution generated from mobile sources is a problem of general interest. In the last 60 years the world vehicle fleet has increased from about 40 million vehicles to over 700million, this figure is projected to increase to 920 million by the year 2010. Due to incomplete combustion of petroleum derived fuels in automobile engines, the exhaust contains various pollutants like CO, HC and NO_x. The reduction of these pollutants before entering into the environment is of greatest concern. The reduction can be done either by engine modification, fuel modification or by exhaust modification. The current practice to eliminate these harmful gases is by using catalytic converters at the tail pipe of the exhaust using noble metals as catalysts. Since the availability and cost of these noble metals do not permit and the costs of these noble metals do not permit them to be used for a long time to come, it is desirable to look into equivalent catalysts which are cheaper and easily available.

Perovskite is a combination of transition and rare earth metals, having the general formula ABO₃, where A is a large cation and B is a small cation. A-cations are believed to be inactive. The partial substitution of A and B-site ions by other metal ions can modify the nature and concentration of defects in perovskite lattice. An A-site substitution by ions in lower valence favors the total oxidation of CO, whereas partial substitution at B-site reinforces the redox property of the perovskite.

In the present study, several catalysts were prepared by the partial substitution of La³⁺ with Ag⁺, Ce⁴⁺, Sr²⁺ and Co³⁺ with Bi⁵⁺ in LaCoO₃ using co precipitation and dry mixing methods and calcined at 800°C. The catalysts were characterized by using XRD, TGA and SEM. The catalytic activity tests were performed in a fixed bed micro size tubular reactor. These tests were conducted in the temperature range of 50-300°C at a constant space velocity of 19850h⁻¹ during all the tests. The exhaust gases from the reactor were analyzed by using a gas chromatograph integrated with the computer.

From the results, the partial substitution of B-site ion with Bi⁵⁺ in LaCoO₃ causes a slight increase in the catalytic activity of the catalyst, but the simultaneous substitutions of both cationic sites enhances the catalytic activity of perovskites for the CO oxidation. Among the simultaneous substituted perovskite catalysts, Ag

substituted catalysts showing best performance in comparison with the Ce and Sr substituted catalysts on which the 100% of CO is obtained at 175°C .

The content of Ag also influences the catalytic activity of substituted perovskites. As the Ag content increases the performance of the catalyst also increases due to the increase in oxygen deficiency in the perovskite lattice. At $x = 0.4$ the complete conversion of CO is observed at 172°C on $\text{La}_{1-x}\text{Ag}_x\text{Co}_{0.8}\text{Bi}_{0.2}\text{O}_{3\pm\delta}$ catalyst. The method of preparation also influences the catalytic activity of the substituted perovskites. The catalysts prepared by co precipitation method showing best performance in comparison with the dry mixing method.

CONTENTS

ACKNOWLEDGEMENT.....	i
ABSTRACT.....	ii
CONTENTS.....	iv
LIST OF FIGURES.....	viii
LIST OF TABLES.....	x
Chapter 1: INTRODUCTION	1
1.1 AUTOMOTIVE EMISSIONS.....	1
1.2 EXHAUST EMISSION CHARACTERISTICS.....	3
1.3 IMPACT OF VEHICULAR AIR POLLUTION ON THE ENVIRONMENT.....	4
1.4 EMISSION REGULATION SCENARIO.....	5
1.5 CONTROL OF VEHICULAR EMISSION.....	6
1.6 CATALYTIC CONVERTERS.....	7
1.7 PEROVSKITE TYPE OXIDES.....	10
1.8 OBJECTIVE OF THE THESIS.....	12
1.9 ORGANIZATION OF THESIS.....	12
Chapter 2: LITERATURE REVIEW.....	13
2.1 GENERAL.....	13
2.2 OXIDATION OF CO.....	13
2.2.1 Simple perovskite oxides.....	13
2.2.2 Substituted perovskite catalysts.....	14
2.3 HC OXIDATION.....	19
2.3.1 Simple perovskite catalysts.....	19
2.3.2 Substituted perovskite catalysts	19

2.4	OXIDATION OF CO AND HC	22
2.4.1	Simple perovskites catalysts.....	22
2.4.2	Substituted perovskite catalysts.....	23
2.5	CHARACTERISTICS OF PEROVSKITES.....	26
2.5.1	Surface composition of perovskites.....	26
2.5.2	Thermal stability.....	27
2.5.3	Sulphur resistance.....	27

Chapter 3: EXPERIMENTAL SETUP AND PROCEDURE.....31

3.1	GENERAL.....	31
3.2	PREPARATION OF $\text{La}_{1-x}\text{M}_x\text{Co}_{1-y}\text{Bi}_y\text{O}_{3\pm\delta}$ (M=Ag, Ce, Sr; x=0, 0.3; y=0, 0.2.....	31
3.2.1	Co precipitation method.....	31
3.2.1.1	Precipitation of metal ions.....	31
3.2.1.2	Heat treatment of catalysts.....	31
3.2.2	Dry mixing method.....	32
3.3	CATALYST CHARACTERIZATION.....	34
3.3.1	X-Ray diffraction analysis.....	34
3.3.2	Scanning electron micrograph.....	34
3.3.4	Thermo gravimetric analysis.....	34
3.4	EXPERIMENTAL SET-UP.....	35
3.4.1	Metering and mixing of feed gases.....	35
3.4.2	Reactor.....	35
3.4.3	Analytical system.....	36
3.5	EXPERIMENTAL PROCEDURE.....	36
3.6	GASCHROMATOGRAPHIC ANALYSIS.....	39
3.6.1	CO analysis.....	39
3.6.2	Propylene analysis.....	39

Chapter 4: RESULTS AND DISCUSSION.....	41
4.1 RESULTS.....	41
4.1.1 Characterization of $\text{La}_{1-x}\text{M}_x\text{Co}_{1-y}\text{Bi}_y\text{O}_{3\pm\delta}$ (M= Ag, Ce, Sr; x=0, 0.3; y=0, 0.2) catalyst.....	41
4.1.1.1 X-ray diffraction pattern.....	41
4.1.1.2 Scanning electron micrographs.....	41
4.1.1.3 Thermal studies.....	41
4.1.2 Catalytic activity studies.....	42
4.1.2.1 Catalytic activity of $\text{La}_{1-x}\text{Ag}_x\text{Co}_{1-y}\text{Bi}_y\text{O}_{3\pm\delta}$ (x=0.0.3; y=0, 0.2) catalysts prepared by co precipitation for CO oxidation.....	42
4.1.2.2 Catalytic activity of $\text{La}_{1-x}\text{Ag}_x\text{Co}_{1-y}\text{Bi}_y\text{O}_{3\pm\delta}$ (x=0.0.3; y=0, 0.2) catalysts prepared by dry mixing method for CO oxidation.....	43
4.1.2.3 Catalytic activity of $\text{La}_{1-x}\text{Ce}_x\text{Co}_{1-y}\text{Bi}_y\text{O}_{3\pm\delta}$ (x=0.0.3; y=0, 0.2) catalysts for CO oxidation.....	43
4.1.2.4 Catalytic activity of $\text{La}_{1-x}\text{Sr}_x\text{Co}_{1-y}\text{Bi}_y\text{O}_{3\pm\delta}$ (x=0.0.3; y=0, 0.2) catalysts for CO and C3H6 oxidation.....	44
4.1.2.5 Catalytic activity of $\text{La}_{1-x}\text{Ag}_x\text{Co}_{0.8}\text{Bi}_{0.2}\text{O}_{3\pm\delta}$ (x=0.1-0.4) catalysts for CO and C3H6 oxidation.....	45
4.2 DISCUSSION.....	59
4.2.1 Effect of A and B-site substitution on the catalytic activity.....	59
4.2.2 Effect of method of preparation on the catalytic activity of $\text{La}_{1-x}\text{Ag}_x\text{Co}_{1-y}\text{Bi}_y\text{O}_{3\pm\delta}$ (x =0, 0.3 and y=0, 0.2).....	60
4.2.3 Effect of Ag content on the catalytic activity of $\text{La}_{1-x}\text{Ag}_x\text{Co}_{0.8}\text{Bi}_{0.2}\text{O}_{3\pm\delta}$ (x =0.1-0.4).....	60

Chapter 5: CONCLUSIONS AND RECOMMENDATIONS.....	62
5.1 CONCLUSIONS.....	62
5.2 RECOMMENDATIONS.....	62
REFERENCES.....	64

LIST OF FIGURES

Fig1.1	Effect of A/F ratio (W/W) on engine emissions end engine power	4
Fig1.2	Conversion efficiency of NO, CO and HC as a function of air fuel ratio in a three way catalytic converter.....	9
Fig1.3	Ideal perovskite structure: a cation at centre of unit.....	11
Fig2.1	Thermal stability of 0.5 Pt/Al ₂ O ₃ and La _{0.9} Ce _{0.1} CoO ₃ for propane oxidation at 600°C	29
Fig3.1	Flow sheet for the preparation of catalyst by Co-precipitation method.....	33
Fig3.2	The schematic representation of the experimental set-up.....	37
Fig 3.3	Photograph of Experimental set-up and fixed bed micro reactor.....	38
Fig 4.1	X-ray diffraction pattern of (a) LaCoO ₃ (b) La _{0.7} Ag _{0.3} CoO _{3±δ} calcined at 800°C.....	46
Fig 4.2	X-ray diffraction pattern of (c) La _{0.7} Ag _{0.3} Co _{0.8} Bi _{0.2} O _{3±δ} (d) LaCo _{0.8} Bi _{0.2} O _{3±δ} calcined at 800°C.....	47
Fig4.3	SEM images of (a) LaCoO ₃ (b) La _{0.7} Ag _{0.3} CoO ₃ catalysts prepared by co-precipitation method and calcined at 800°C at 10KX.....	48
Fig 4.4	SEM images of (c) La _{0.7} Ag _{0.3} Co _{0.8} Bi _{0.2} O ₃ (b) LaCo _{0.8} Bi _{0.2} O ₃ catalysts prepared by co-precipitation method and calcined at 800°C at 10KX.....	49
Fig 4.4	Thermo Gravimetric (a), Differential Thermal (b), Derivative Thermo Gravimetric (c) analysis of (1) LaCoO ₃ , (2)La _{0.7} Ag _{0.3} CoO ₃ catalysts.....	50
Fig 4.5	Thermo Gravimetric (a), Differential Thermal (b), Derivative Thermo Gravimetric (c) analysis of (3) La _{0.7} Ag _{0.3} Co _{0.8} Bi _{0.2} O ₃ , (4)LaCo _{0.8} Bi _{0.2} O ₃ catalysts.....	51

Fig 4.6	Comparison of catalytic activity of $\text{La}_{1-x}\text{Ag}_x\text{Co}_{1-y}\text{Bi}_y\text{O}_{3\pm\delta}$ ($x = 0, 0.3; y = 0, 0.2$) catalysts prepared by co-precipitation method and calcined at 800°C for CO oxidation ...	52
Fig 4.8	Comparison of catalytic activity of $\text{La}_{1-x}\text{Ag}_x\text{Co}_{1-y}\text{Bi}_y\text{O}_{3\pm\delta}$ ($x = 0, 0.3; y = 0, 0.2$) catalyst prepared by dry mixing method for the oxidation of CO	53
Fig 4.9	Comparison of catalytic activity of $\text{La}_{1-x}\text{Ce}_x\text{Co}_{1-y}\text{Bi}_y\text{O}_{3\pm\delta}$ ($x = 0, 0.3; y = 0, 0.2$) catalyst prepared by co-precipitation method for the oxidation of CO.....	54
Fig 4.10	Comparison of catalytic activity of $\text{La}_x\text{Sr}_{1-x}\text{Co}_y\text{Bi}_{1-y}\text{O}_{3\pm\delta}$ ($x = 0, 0.3; y = 0, 0.2$) catalyst prepared by co-precipitation method for the oxidation of CO.....	55
Fig 4.11	Comparison of catalytic activity of $\text{La}_x\text{Sr}_{1-x}\text{Co}_y\text{Bi}_{1-y}\text{O}_{3\pm\delta}$ ($x = 0, 0.3; y = 0, 0.2$) catalyst prepared by co-precipitation method for the oxidation of C_3H_6	56
Fig 4.12	Comparison of catalytic activity of $\text{La}_x\text{Ag}_{1-x}\text{Co}_{0.8}\text{Bi}_{0.2}\text{O}_{3\pm\delta}$ ($x = 0.1- 0.3$) catalyst prepared by co-precipitation method for the oxidation of CO.....	57
Fig 4.13	Comparison of catalytic activity of $\text{La}_x\text{Ag}_{1-x}\text{Co}_{0.8}\text{Bi}_{0.2}\text{O}_{3\pm\delta}$ ($x = 0.1- 0.3$) catalyst prepared by co-precipitation method for the oxidation of C_3H_6	58
Fig 4.14	The temperature of 50% CO conversion as a function of Ag content in $\text{La}_{1-x}\text{Ag}_x\text{Co}_{0.8}\text{Bi}_{0.2}\text{O}_{3\pm\delta}$	61

LIST OF TABLES

Table 1.1	Mass emission characteristics of different type of vehicle.....	2
Table 1.2	Shows the emissions per day of different type of vehicles.....	2
Table 1.3	Health effects of common vehicular air pollutants.....	5
Table 3.1	Calcination temperature and heating schedule in the preparation of perovskite oxides by co-precipitation method.....	32
Table 3.2	Specifications for thermal analysis.....	35
Table 3.3	GC conditions for CO analysis.....	40
Table 3.4	GC conditions for C ₃ H ₆ analysis.....	40
Table 4.1:	Characteristic conversion temperatures for CO oxidation on La _{1-x} Ag _x Co _{1-y} Bi _y O _{3±δ} (x =0, 0.3; y=0, 0.2) catalyst prepared by co-precipitation	42
Table 4.2	Characteristic conversion temperatures for CO oxidation on La _{1-x} Ag _x Co _{1-y} Bi _y O _{3±δ} (x =0, 0.3; y=0, 0.2) catalyst prepared by dry-mixing method.....	43
Table 4.3	Characteristic conversion temperatures for CO oxidation on La _{1-x} Ce _x Co _{1-y} Bi _y O _{3±δ} (x =0, 0.3; y=0, 0.2).....	44
Table 4.4	Characteristic conversion temperatures for CO and C ₃ H ₆ oxidation on La _{1-x} Sr _x Co _{1-y} Bi _y O _{3±δ} (x =0, 0.3; y=0, 0.2).....	45
Table 4.5	Characteristic conversion temperatures for CO and C ₃ H ₆ oxidation on La _x Ag _{1-x} Co _{0.8} Bi _{0.2} O _{3±δ} (x =0.1- 0.4)	45

INTRODUCTION

Over the course of the past fifty years, the vehicle population around the world has exploded. The majority of these vehicles employ combustion of fuels derived from crude oil as the main source of energy in their engines. Due to non-perfect combustion and the high temperatures reached in the combustion chamber, the exhaust contains significant amount of pollutants like CO, HC and NO_x ...etc which need to be transformed in to harmless products. The current practice to eliminate these harmful gases is by using catalytic converters at the tail pipe of the exhaust using noble metals as catalysts. Since the availability and cost of these noble metals do not permit them to be used for a long time to come, it is desirable to look into equivalent catalysts which are cheaper and easily available.

The objective of the present project is, therefore, screen suitable catalysts based on non-noble metals. Automobiles are the major source of pollution in mega cities of our country. The present work has been aimed to eliminate CO from automotive exhaust employing catalytic converters as CO is the major pollutant emitted from a gasoline engine.

1.1 AUTOMOTIVE EMISSIONS

The exhaust from the automobile consists of various air pollutants. Among these pollutants emitted from automobiles, the major air polluting materials are classified as follows:

- Gaseous substances: NO_x, SO_x, CO, unburnt hydrocarbons, and aldehydes etc.
- Aerosols: smoke and mist consisting of particulate materials, such as, carbon particles, unburnt or partially burnt fuel molecules and polymerization products.
- Odour (mainly due to aldehydes)
- Carcinogens: polynuclear aromatic hydrocarbons such as benzopyrene and benzoanthracene.
- Lead and other metals (blended with the fuel as anti-knocking or anti-corrosive agents) in vaporous and particulate form.

The estimated vehicular mass emission contribution in India in the year 1992-93 was about 1.735 million tonnes of carbon monoxide (CO), 0.8 million tonnes of hydrocarbons (HC) and 0.85 million tonnes of nitrogen oxides (NO). Gasoline (petrol) driven vehicles are found to be responsible for around 97 percent of CO and hydrocarbons emission. Gasoline vehicles also contribute 32 percent of total NO_x emissions and 15 percent of SO_x emissions. Diesel vehicles emit smoke comprising of suspended particles, HCs and NO_x. Table 1.1 presents the mass emission characteristics of different types of vehicles in India and Table 1.2 give the current and the projected vehicular pollution loads in the country.

Table 1.1: Mass emission characteristics of different type of vehicles.

S.No	Vehicle Type	CO	HC	NO _x
1.	Petrol driven			
	(a) Cars(four stroke engine)	240	31	16
	(b) Mopeds	304	215	1.8
	(c) Scooters/Motor cycle(two/four stroke Engine) ?	257	161	1.8
2.	Diesel vehicles (?)	19	8	37

Units: gram/liter of fuel consumed

Table 1.2: Emissions per day of different type of vehicles

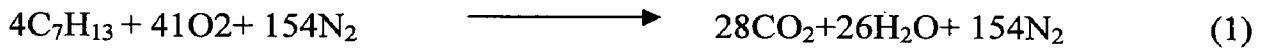
Year	2-Wheeler	3-Wheeler	Cars	MUVS	CVES	Total
1986	1134	912	1112	1059	5775	9992
1991	2598	1787	1985	2004	9528	17901
1996	4486	2923	2377	2099	11943	23828
2000	5775	4910	2562	2282	12272	27800

Units: Tonnes emission per day (CO+HC+NO_x+PM)

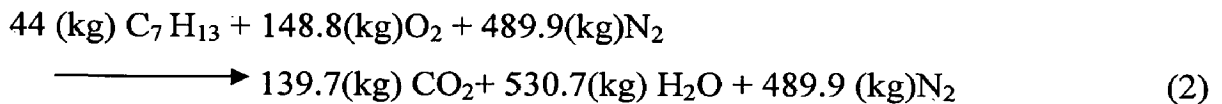
1.2 EXHAUST EMISSION CHARACTERISTICS

Emissions from gasoline powered vehicles are generally classified as: (a) Exhaust emissions, (b) Crank-case emissions and, (c) Evaporative emissions. The amount of pollutants that an automobile emits depends on a number of factors, including the design and operation (idle, acceleration, etc.). Of the hydrocarbons emitted by a car with no controls, the exhaust gases account for roughly 65%, evaporation from fuel tank and carburetor for roughly 15% and crank-case emission (gases that escape around the piston rings) for about 20%. CO, NO_x and lead compounds are emitted almost exclusively in the exhaust gases.

Petrol consists of a mixture of various hydrocarbons. Considering petrol as C₇H₁₃, combustion of petrol to carbon dioxide occurs according to the following equation (Central Pollution Control Board (CPCB), CUPS/17/1988):



On mass basis, equation (1) can be written as:



The composition of exhaust varies according to the air/fuel ratio as shown in fig 1.1 for a standard gasoline fuel where the A/F ratio is around 14.7. If the A/F ratio is below 14.7 the exhaust contains high amounts of unburnt hydrocarbons and carbon monoxide due to incomplete combustion. If it is more than 14.7 the concentration of nitrogen oxides and hydrocarbons is high in the exhaust due to unstable combustion.

In spark ignition engines, complete combustion does not take place since the spark induced reaction is not fully propagated inside the piston chamber. The incomplete combustion products including CO and NO_x are produced even at stoichiometric A/F ratio.

In actual practice, two- and three-wheeler petrol engines have low A/F mixture (A/F=12) during cold start, idling, acceleration and high speed cruising and similarly diesel engines receive low air to fuel ratio (A/F=16) when running at a medium speed. The air supplied for combustion contains about 77% of nitrogen. At temperatures higher than 600°C nitrogen reacts with oxygen, and, therefore, during combustion process some amount of NO_x is formed.

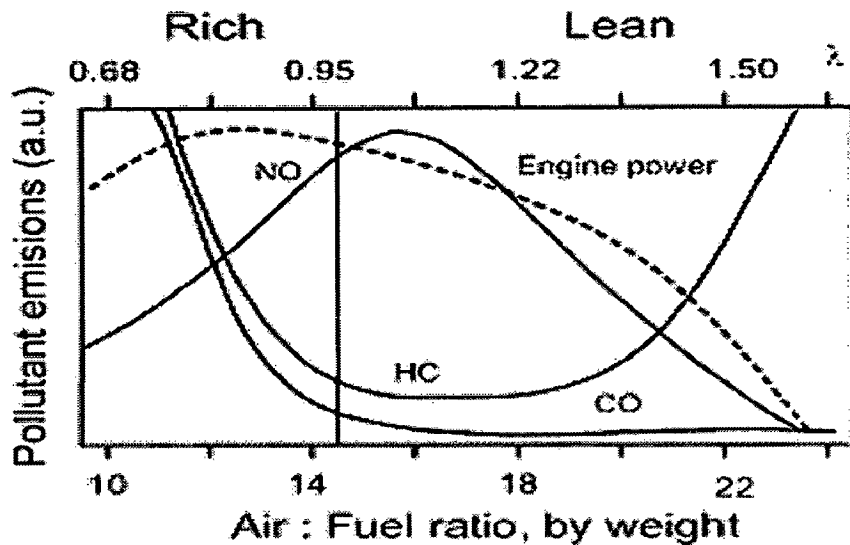


Fig1.1 Effect of A/F ratio (w/w) on engine emissions and engine power

Ref. ?

The characteristics of exhaust emissions from two-stroke motor-cycles and those from automobiles are significantly different. For two-stroke motor cycles, the air/fuel (A/F) ratio monotonously decreases with increasing engine speed from A/F >14.63 (stoichiometric point) at the idle speed to A/F < 11.0 at a high engine speed or heavy load, whereas for automobiles the A/F ratio hovers around the stoichiometric point [Lee and Chen, 1997]. This lowering of A/F ratio in two-stroke motor cycles results in increased emission levels for CO, HC in comparison to automobiles. Also, NO_x emitted by two-stroke motor cycles is almost insignificant (<0.1 g/km), whereas CO and HC emissions are very large- 5% and 5000 ppm (v/v), respectively [Mooney et al, 1975].

1.3 IMPACT OF VEHICULAR AIR POLLUTION ON THE ENVIRONMENT

The various air pollutants emitting from automobiles cause severe health problems to human beings. Among these air pollutants carbon monoxide is very harmful to human beings and animals. It has 250 times greater affinity to haemoglobin than that of oxygen and it reacts and neutralizes a part of haemoglobin in the blood, thus reducing respiratory capacity. When in a large concentration of 100 ppm or more, it can cause death with relatively short exposure. Oxides of nitrogen and the nitrated organics and oxidants generated due to them are considered to be the most hazardous. Even small

quantities of these chemicals cause lachrymation (burning of eyes, noses, other delicate membranes of the body), may be carcinogenic in long term, affect and destroy plant tissue and may attack even such resistant materials as rubber, nylon and plastics. In urban areas the most noticeable effect of vehicular air pollution is the reduction in visibility. Photochemical smog, the product of complex chemical reaction in the atmosphere gives rise to the familiar haze and to vegetation damage, eye irritation and respiratory distress. Particulates, pose a hazard to the health of animal and plant kingdoms and also to the longevity of the structure and property. Table 1.4 summarizes the effect of vehicular air pollutants on human health.

Table 1.3: Health effects of common vehicular air pollutants

Ref. 7

Emissions	Short term health effects	Long term health effects
CO	Asphyxiation	Fetal at COHb level of 2-5%
HC	Difficulty in breathing	Impaired lung function
NOx	Sourness and cough	Lung cancer
SO2	Asthma	Lung cancer
Particulates	Asthma	Selicexis(Brown lung)
Inorganic Lead Compounds	Affects kidney and GI Function	Mental impairment

1.4 EMISSION REGULATION SCENARIO

Auto-exhaust emission control over the whole world has been achieved by stipulating emission standards and implementing them. The Ministry of Environment and Forests, Govt. of India [1990] has framed certain regulations to regulate vehicular emissions. Some of the provisions are detailed below:

- (1) Every motor vehicle shall be manufactured and maintained in such condition and shall be so driven that smoke, visible vapor, grit, sparks, ashes, cinders or oily substance do not emit therefrom.
- (2) On and from the 1st day of March 1990, every motor vehicle in use shall comply with the following standards:-

- (a) Idling CO (carbon monoxide) emission limit for all four wheeled petrol driven vehicles shall not exceed 3 percent by volume;
 - (b) Idling CO emission limit for all two and three wheeled petrol driven vehicles shall not exceed 4.5 percent by volume;
- (3) On and from the 1st day of April, 1991, all petrol-driven vehicles shall be so manufactured that they comply with the mass emission standards as specified by the Ministry of Environment and Forestry, Govt. of India.
- (4) Each motor vehicle manufactured on and after the dates specified in paragraphs 2 & 3 above, shall be certified by the manufacturers to be conforming to the standards specified in the said paragraphs and the manufacturers shall further certify that the components liable to effect the emission of gaseous pollutants are so designed, constructed and assembled as to enable the vehicle, in normal use, despite the vibration to which it may be subjected, to comply with the provisions of the said paragraphs.

With a view to reduce the emission load of pollutants in India too, emission regulations for the year 2005 have already been notified and for the year 2010 still tougher Standards are being proposed.

1.5 CONTROL OF VEHICULAR EMISSION

Three approaches are normally adopted for the pollution control from Automobiles:

- (1) **Engine modification:** which employs suitable modification of the internal combustion engine for the reduction in the amount of pollutants formed during combustion or replacements of internal combustion engine with low pollution producer engine
- (2) **Fuel modification:** which employs development of suitable fuel for petrol and leaded petrol like natural gas that will produce low levels of pollutant after combustion?

- (3) **Exhaust modification**: which employs development of exhaust system reactor(catalytic converter) that will complete the combustion process and change the potential pollutants into more acceptable materials.

Engine modification yields only moderate reduction and penalties on engine performance and fuel efficiencies are substantial. Fuel modification or substitution and replacement of spark ignition engines for all the petrol driven vehicles in India are not feasible at present. Exhaust treatment seems to be the only answer at present which can be achieved through one of the two systems, thermal reactor package and catalytic converter package

The thermal reactor package relies on homogeneous oxidation of fuel components to control CO and HC emission. Catalytic converter package uses catalysts for the conversion of CO and HC into CO₂ and H₂O.

1.6 CATALYTIC CONVERTERS

Catalytic converters normally use three types of catalysts:

- (1) Oxidation catalysts for CO and HC.
- (2) Dual catalysts, which incorporate in series a reduction catalyst for NO_x and an oxidation catalyst for CO and HC.
- (3) Three-way catalysts for the oxidation of CO, HC and the reduction of NO_x

With the first two methods, exhaust gas recirculation (EGR) is to be added to the system for NO_x control.

Apart from other methods, the incorporation of catalytic converter in the exhaust system is most promising in meeting the increasingly rigid emission regulations. The use of noble metal based catalytic converters have shown tremendous success in reducing pollution levels from the exhaust. These converters have, however, shown their efficiency with high octane unleaded petrol.

The catalytic converter approach has several advantages as it can be easily placed in existing vehicles without much of modifications in the engine, it does not require decoupling of emission control from engine operation; it has very high (95%) conversion efficiencies; and it does not need costly heat resistant materials. Figure 1.2 shows the conversion efficiency of NO_x, CO and HC as function of the air-fuel ratio.

Generally, the catalysts used in the converters are classified as follows:

- (i) Supported catalysts based on noble metal catalysts such as Pt, Pd, Rh supported on alumina and their promoted versions.
- (ii) Transition metal oxide catalysts such as Cu, Co, Ni, Fe, Cr, V, Mn and promoted versions of these materials.
- (iii) Unsupported metallic alloys - like monel metal (66.5% Ni, 31.5% Cu, 2.1% others)

The catalyst chosen for vehicle emission control should satisfy certain conditions, namely, it should be cheap and readily available; should be effective for wide range of temperature (from ambient to 900°C); must be able to withstand thermal shock; must convert combustion products into harmless products; should have high conversion efficiency; should withstand the poisoning action of additives in the fuel that are emitted in the exhaust; should be attrition resistant to highly turbulent flows through the converter; and should also be operational for around 80,000 km run of the vehicles with high efficiency.

However, the catalytic converters also have a number of drawbacks. The catalysts are active only at relatively high temperatures, during warm up periods, heavy emissions normally take place. The catalysts operate over a wide but not unlimited temperature range and temperature control is required to avoid burn-out temperature at high speeds and high loads. The catalysts are poisoned by exhaust constituents, in particular by lead and sulfur compounds, hence conversion efficiency decreases with the period of use. The catalytic bed in the converter system, often, offers considerable back pressure which increases with time of use.

Catalytic converter operation is generally handicapped due to oxygen deficiency in two-stroke motor cycle operation. HC conversion efficiency increases with temperature, whereas CO conversion is favoured at lower temperatures in oxygen-rich environment. At higher speeds, with exhaust temperature rising and oxygen concentration depleting, CO conversion is adversely affected. Thus, the control of CO and HC emissions simultaneously is a difficult task.

The Otto engine and diesel engine each require a different approach to the catalytic cleaning of their exhaust gases. Diesel engines are inherently more cleaner than

petrol driven engines (Otto engines) from the standpoint of carbon monoxide (CO) and hydrocarbons (HC) emissions. Taking into account the much greater petrol driven vehicular fleet (because of 2/3 wheelers - scooters, motor cycles and auto rickshaws) research in India is being focussed on reducing CO/HC levels in the first phase. Noble metals are very costly and are in limited supply. This inhibits their use in catalytic converters, and has spurred serious efforts to find substitutes of noble metals. Systems based on base metals like Cu, Cr, Co, Ni etc. are cheaper. However, these metals are relatively inactive and susceptible to poison by sulfur compounds and H₂O. The catalysts are ineffective until they reach the light-off temperature (i.e. the temperature at which 50% of the component in question reacts or is converted to an acceptable gas).

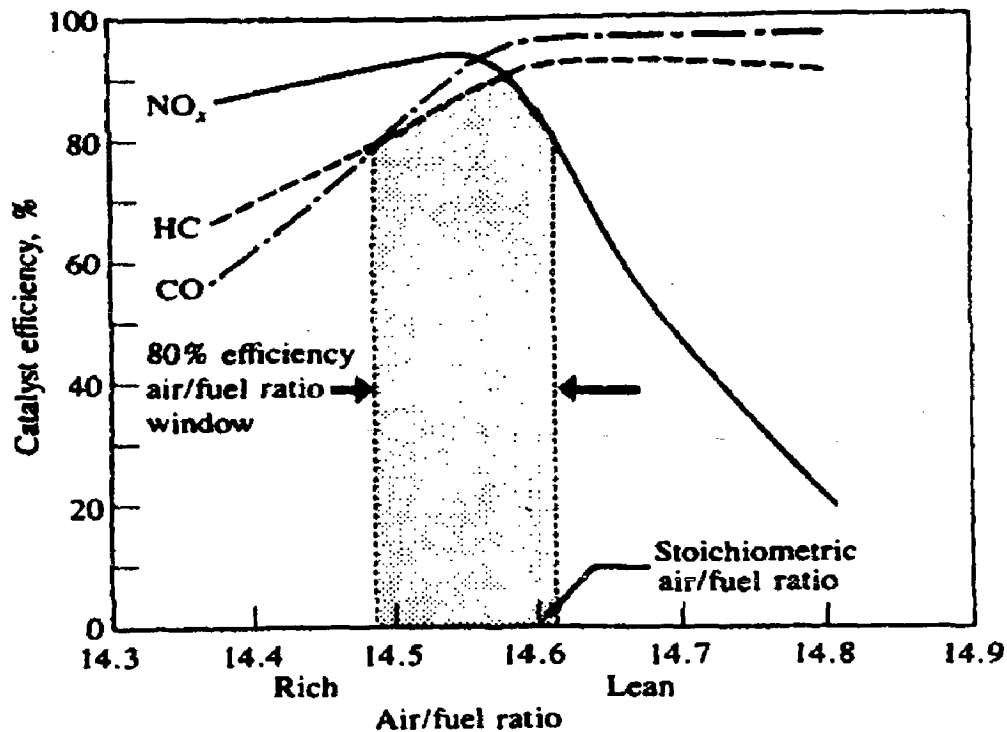


Fig 1.2 Conversion efficiency of NO, CO and HC as a function of air fuel ration in a Three Way Catalytic Converter

1.7 PEROVSKITE TYPE OXIDES

Perovskites are represented by oxides having a general form ABX_3 , where A is a large cation, B is a smaller cation, and X is an anion; in cases of interest of this work, X is oxygen. Fig. 1.3 shows a unit cell of the ideal perovskite structure with the B cation at the origin and A cation at the center. Galasso (1960) has found that very few perovskite-type oxides have exactly the ideal cubic structure at room temperature, but may assume this structure at higher temperatures also.

In the perovskite structure, the A cation is coordinated with twelve oxygen ions and the B cation is coordinated with six. In order to have contact between the AB and O cations, Goldschmidt (1926) defined a tolerance factor:

$$t = (R_A + R_O) / 2^{0.5} (R_A + R_B)$$

Here R_A , R_B , and R_O are the corresponding ionic radii. By geometry the ideal cubic structure correspond to $t = 1$. Actually the structure occurs in the range of t equal to $0.75 < t < 1.00$. For distorted perovskite structures a somewhat larger range of the tolerance factor is allowable. Goodenough and Longo (1970) have noted that the Goldschmidt tolerance factor, shown in the above mentioned equation is not a sufficient condition for a stable perovskite structure because in oxides the A cation is coordinated to twelve oxygen ions and the B cation to six, which sets lower bounds for the cation radii. These bounds for oxides are $R_A > 0.90 \text{ \AA}$ and $R_B > 0.51 \text{ \AA}$.

Besides the ionic radii requirements, the other condition to be fulfilled is electroneutrality, i.e. the sum of charges of A and B ions equal to total charge of X anions. This is attained in the case of oxides by means of charge distribution of the form $A^{1+} B^{5+} O_3$, $A^{2+} B^{4+} O_3$, or $A^{3+} B^{3+} O_3$. Moreover partial substitution of A and B ions giving rise to complex oxides is possible while keeping the perovskite structure.

The valence state of B ion in ABO_3 can be changed by partial substitution at A or B site with ions having different valences. Partial replacement of host A cations in ABO_3 induces several electronic and ionic defects in the bulk of perovskites and it naturally affects the catalytic properties. Extensive investigation on A-site substitution perovskites have been carried out for the purpose of basic understanding as well as for practical purposes. The substitutes (A) for trivalent rare earth cations include univalent (K, Ag), divalent (Ca, Sr, Ba) and tetravalent (Ce, Hf) cations. The partial substitution of foreign

B' metal for B-site can produce a defect structure which influences catalytic properties, as is the case in A-site partial substitution. In addition a strong synergetic effect can often be produced in this case by mixing two B-site components which are both catalytically active. By partial substitutions at both position A, B- sites we can produce a catalyst with different catalytic properties.

In early seventies cobaltate perovskites were suggested as substitute for noble metals in automotive exhaust catalysis and in electro catalysis. Encouraging results were obtained with cobalte and manganate perovskites in the oxidation of carbon monoxide (CO) and the reduction of nitric oxide (NO). At low CO concentrations, representative of a large degree of conversion of CO in auto exhaust, the activity of the manganates and cobaltates is significantly less than that of Pt. However the susceptibility of these perovskites to sulfur dioxide damped the initial enthusiasm for their application in automotive exhaust catalysis.

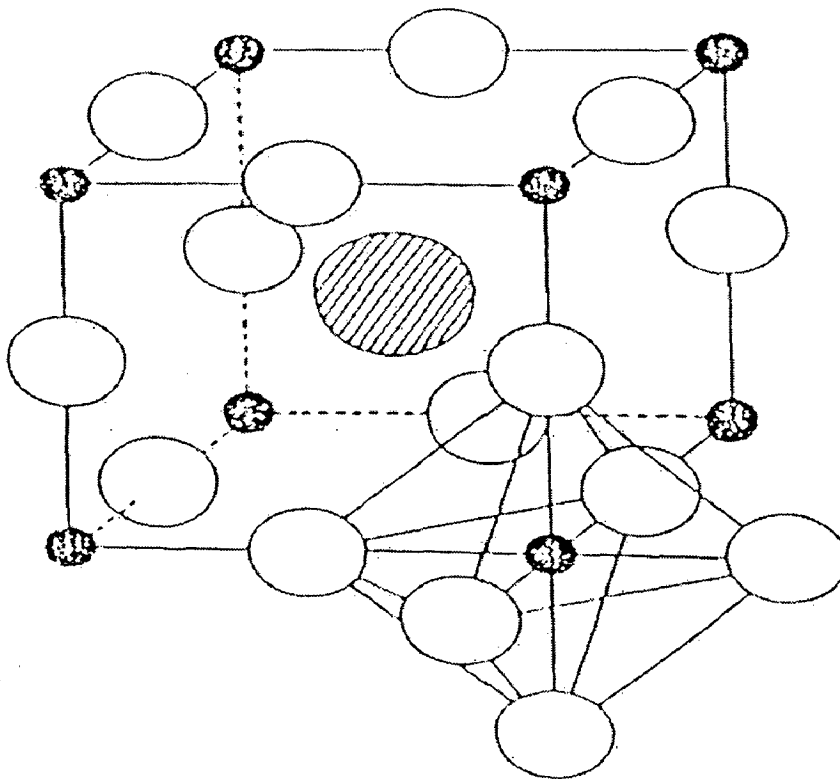


Fig1.3 Ideal perovskite structure: A cation at centre of unit

The perovskite exhibit improved resistance against heat and reduction, have good mechanical shock –resistance capabilities, have higher resistance against lead poisoning, and are cheap. These properties propel the perovskites to be used as oxidation catalysts in pollution emission control. The perovskites have low specific surface area and are susceptible to poisoning by sulfur. So these problems have to be solved before perovskite find much application as oxidation catalysts.

Few studies on perovskite catalysts for CO and HC oxidation were made with the substitutions at either A or B sites in the perovskite structure. In the present work we plan to study the activity of perovskite catalysts by partial substitution at both positions (A, B-sites) simultaneously.

1.8 OBJECTIVE OF THE THESIS

The objective of the present study is set as follows:

- (i) Synthesis of LaCoO_3 and its A-site and B-site substituted forms, (with Ag, Ce, Sr and Bi) by using co-precipitation and dry mixing methods and their characterization using X-ray diffraction, thermo gravimetric analysis, etc.
- (ii) Studies on the performance of the synthesized catalysts for the oxidation of CO using synthetic gas mixture.

1.9 ORGANIZATION OF THESIS

Chapter I includes the introduction of thesis, brief description about automotive emissions, emission control technologies, catalytic converter and objective of the thesis. Chapter II gives a brief literature review. Chapter III includes method preparation of catalysts, details of experimental set up and experimental procedure. Chapter IV consists of results and discussion. Chapter V gives concluding remarks and recommendations for future work.

LITERATURE REVIEW

2.1 GENERAL

In this chapter, a review of the existing literature, to the extent available, on the perovskite based mixed oxides and its substituted forms, both at A-site and B-site, their characteristics, and their performance for the oxidation of CO and hydrocarbons towards automotive exhaust pollution control has been presented.

2.2 OXIDATION OF CO

2.2.1 SIMPLE PEROVSKITE OXIDES

Libby (1970) suggested that LaCoO_3 , a p-type semiconductor, might be a good catalyst for the treatment of automotive emission which would be cheaper than the noble metal catalysts such as platinum. This suggestion has been followed by a number of researchers for the development of catalytic converters which would promote reduction of NO with CO to yield N_2 and CO_2 , and the air oxidation of CO and HC to yield CO_2 and H_2O respectively.

Simonot *et al* (1997) prepared LaCoO_3 , Co_3O_4 and a mixture of them, and studied the activities for the automotive exhaust reactions. Two preparation methods were used: simultaneous precipitation and sol-gel type. The samples were characterized by X-ray diffraction, TPR, TPO and microanalysis. The CO oxidation reaction was performed under dry or wet atmospheres for a binary ($\text{CO} + \text{O}_2$) and complete ($\text{CO} + \text{NO} + \text{C}_3\text{H}_8 + \text{O}_2$) gas mixture. In all cases, cobalt oxide exhibited the best performance. A quenching effect of the surface of the sol-gel catalysts induced activity at room temperature under the ($\text{CO} + \text{O}_2$) dry mixture. Under the complete wet gas mixture, the perovskite LaCoO_3 showed lower activation energy for the CO oxidation reaction than for Co_3O_4 .

2.2.2 SUBSTITUTED PEROVSKITE CATALYSTS

Voorhoeve *et al* (1972) conducted tests for CO oxidation on the compounds $RE_{1-x}Pb_xMnO_3$ and $RECoO_3$. RE (rare earth) is lanthanum, praseodymium or neodymium. $Nd_{1-x}Pb_xMnO_3$ and $PrCoO_3$ were found to be more active than platinum catalyst. Other manganites and cobaltites were approximately as active as the platinum catalyst. Johnson *et al.* (1973) tested a number of rare earth perovskite formulations of basic composition ABO_3 , where A is rare earth (RE) or mixture of RE, Pb, Ca, Sr or Ba, and B is Co or Mn. For CO oxidation, $La_{0.5}Sr_{0.5}MnO_3$ was found to be most active. Etching with 5% nitric or hydrochloric acid improved the activity of these catalysts.

Johnson *et al* (1973) prepared a number of rare earth perovskite formulations of basic composition ABO_3 , where A is rare earth (RE) or mixture of RE, Pb, Ca, Sr or Ba and B is Co or Mn. In the conventional procedure i.e. ceramic method, by dry mixing and calcination at $1000^\circ C$, catalyst of 1 to 2 m^2/g surface area were produced. By precipitation of nitrate of respective materials using ammonia solution, surface area in the range of 5 to 45 m^2/g was found. Calcination temperature of $800^\circ C$ and lower were employed. These catalysts were tested for CO oxidation and $La_{0.5}Sr_{0.5}MnO_3$ was found most active. Etching with 5% nitric or hydrochloric acid improves the activity of these catalysts.

Johnson *et al* (1976) compared CO oxidation for $LaMn_{0.5}Cu_{0.5}O_3$ prepared by three methods: freeze drying, spray drying and precipitation. The catalytic activities were in the order; Freeze-drying > Spray-drying > Precipitation. This could be due, in part, to the differences in the calcination temperature (i.e., mere change in the calcination temperature would change the surface properties of these oxides). When the activities were normalized to the surface area, the differences became smaller, but the order remained the same.

Voorhoeve *et al* (1977) brought forward new ideas in explaining the role of defect chemistry of perovskites, such as, cobaltites, manganites, chromites and ruthenates. They suggested that the catalysis of perovskite-type oxide should be divided into two types: interfacial - and superficial catalysis. In the interfacial catalysis, the removal of oxygen from the lattice of the catalyst plays an important role. So, the reaction is controlled primarily by the thermodynamics of reduction and oxidation of the

oxide bulk. On the other hand, superficial catalysis proceeds with the reaction between adsorbed species on the surface. In this case, the rate is mainly controlled by the electronic configuration of the transition metal ions on the surface. According to them, CO oxidation at high temperatures (380 - 500°C) is an example of interfacial catalysis, whereas, CO oxidation at low temperatures (100 -200°C) is superficial. Although no substantial evidence has been presented, this classification appears to be useful. It has been indicated that a similar transition between the two mechanism is also brought about by the valency control; possibly superficial for LaCoO_3 and interfacial for $\text{La}_{0.6}\text{Sr}_{0.4}\text{CoO}_3$.

Gallagher *et al.* (1977) studied the catalytic activity of $\text{La}_{0.7}\text{Pb}_{0.3}\text{MnO}_3$ having various Pt content for CO oxidation. The effect of Pt at a level of 570 ppm or less was small, but at 1600-5500 ppm level, Pt increased the activity significantly.

Tabata *et al.* (1986) examined the thermal stability of $\text{La}_{0.9}\text{Ce}_{0.1}\text{CoO}_3$ (prepared by calcination at 850°C). After catalyst was heated in air at 800°C for various periods in a mantle heater, the catalytic activities were measured for the oxidation of CO at 600°C. It has been found that the catalytic activity of $\text{La}_{0.9}\text{Ce}_{0.1}\text{CoO}_3$ did not change at all even after 1000 hrs life test, although the activity of the Pt catalyst dropped significantly.

Wan *et al.* (1987) prepared a properly designed perovskite-type base metal catalyst $\text{La}_{0.6}\text{Sr}_{0.4}\text{Co}_{1-x}\text{M}_x\text{O}_3$ which had certain SO_2 resistant properties. Over this catalyst, at 56000 h^{-1} space velocity, CO could be oxidized at 100% in the presence of 20, 200, and 400 ppm of SO_2 at 200°, 300°, 400°C, respectively. The deactivation of the catalyst by 50 and 400 ppm of SO_2 at 200°, 300°C, respectively, was found to be reversible. IR spectroscopy revealed that SO_2 was adsorbed on B site ions which deactivate the catalyst by blocking the surface sites that were necessary for CO adsorption and lattice oxygen replenishment. A comparison was made with another $\text{La}_{0.6}\text{Sr}_{0.4}\text{CoO}_3$, which was found to be more susceptible to SO_2 poisoning. Mizuno *et al.* (1989) studied the effects of the substitution at the B-site in $\text{LaMn}_{1-x}\text{Cu}_x\text{O}_{3-y}$ catalyst and obtained very high activities for the oxidation of CO for $0.4 < x < 0.7$. This synergetic effect was presumably ascribed to an appropriate combination of the activation of CO by Cu and reactive oxygen related to Mn oxide, based on the data of CO adsorption and thermal desorption of oxygen. Chan *et al.* (1994) tested $\text{La}(\text{Mn,Cu})\text{O}_3$, $(\text{La, Sr})\text{CoO}_3$ and

(La,Ce)CoO₃, catalysts for CO oxidation and found La_{0.8}Sr_{0.2}MnO₃ most active above 200°C temperature.

A fascinating result was obtained with LaMn_{1-x}Cu_xO₃ system, in which Cu substitution markedly enhanced CO oxidation activity, although no positive effect was confirmed in the case of propane oxidation. The rate of CO oxidation on the most active LaMn_{0.6}Cu_{0.4}O₃ was about 400 and 5000 times larger than that on the end members, LaMnO₃ or La₂CuO₄, respectively, and hundred times larger than that on La_{0.8}Sr_{0.2}CoO₃ and Pt/Al₂O₃. A synergetic effect between Cu and Mn was assumed; Cu promotes the activation of Co while Mn promotes the reactivity of lattice oxygen.

Zhang *et al* (1987) prepared several substituted perovskite catalysts using citric acid for the oxidation of Co. The surface area produced by this method was 44.8 m²/g. on the other hand in the case of Sr containing perovskites, especially with high Sr contents, strontium nitrate was converted to strontium carbonate above 550°C and single phase oxide was obtained only after calcination above 800°C.

Mizuno *et al* (1988) prepared LaMn_{1-x}Cu_xO_{3-y} from the solution of the nitrates or acetates were single phase perovskites up to x=0.6. The composition of those from acetates was more nearly uniform, resulting in much higher activities. Very high activities for the oxidation of CO were obtained for 0.4<x<0.7. This synergetic effect was presumably ascribed to an appropriate combustion of the activation of CO by Cu and reactive oxygen related to Mn oxide, based on the data of CO adsorption and thermal desorption of oxygen.

Du *et al* (1993) investigated a series of Ni-substituted LaMnO₃ catalyst for the effect of Ni substitution on the crystal structure of the catalysts and their catalytic activities of CO oxidation. XRD showed that the samples of LaMn_{1-x}Ni_xO₃ catalysts for x= 0.0-0.4 and 0.8- 1.0 had rhombohedral symmetry, and for x = 0.5-0.8 it had pseudo-cubic symmetry. Usually transition metal perovskite oxides having cubic symmetry show only two strong IR absorption peaks in the 400-800 cm⁻¹ bands which are assigned to octahedral BO₆ group (Blasse *et al.*, 1973). But for x = 0.5-0.8 appearance of three absorption bands in this region is ascribed to lower symmetry of the lattice or the presence of different types of Ni and Mn ions. From this effect they concluded the existence of interactions between Mn and Ni ions coexisting in the B sites of ABO₃. TPR

analysis showed a decrease in reductive stability with the increase of substitution of Ni except for $x = 0.4$ and 0.8 which are ascribed to the region of symmetry transition. The order of catalytic activity for CO oxidation is $x = 0.5 < 0.6 < 0.8$ for pseudo-cubic samples, and for rhombohedral sample, it is $x = 0.4 > 1.0$. The reason for such behavior is ascribed to the weakening of B-O band due to symmetry transition which makes lattice oxygen highly active at temperatures higher than 310°C .

Chan *et al* (1994) studied the influence of either A or B-site substitution in perovskite-type mixed oxides on the catalytic oxidation of carbon monoxide. The following systems were investigated: $(\text{La,Sr})\text{MnO}_3$, $\text{La}(\text{Mn,Cu})\text{O}_3$, $(\text{La,Sr})\text{CoO}_3$ and $(\text{La,Ce})\text{CoO}_3$. Cobaltates are generally more active than the manganates. Substitution in the A or B-site improved the catalytic activity with oxidation starting from 75°C . A volcano plot of activity versus composition was obtained for each series with up to a 10-fold increase in catalytic activity for the substituted compounds. Lattice oxygen participates in the reaction even under stoichiometric conditions. The catalysts show a positive rate dependence on the carbon monoxide partial pressure so that under reducing conditions, the reaction is not inhibited. A bi-stability in the rate of catalytic oxidation at higher carbon monoxide concentration was observed over $\text{La}_{1-x}\text{Sr}_x\text{MnO}_3$ and $\text{LaMn}_{1-x}\text{Cu}_x\text{O}_3$ ($0 < x < 0.2$). This bi-stability has been attributed to a carbon monoxide-driven reconstruction of the reduced surface, leading to pairs of Mn^{2+} ions with a Mn-Mn distance comparable to the spacing in the metal. These pairs provide reactive sites for carbon monoxide oxidation and oxygen chemisorption. Such metal-metal pairs are not found in the perovskite lattice but are a structural feature of the closely related hexagonal 4-layered packing which is the normal crystal structure of SrMnO_3 . The change back to the less active state is due to reoxidation of the surface. It was confirmed that a low mobility of lattice oxygen was a necessary condition for hysteresis in these oxides.

Dai *et al* (2001) investigated the perovskite catalyst $\text{La}_{0.8}\text{Ba}_{0.2}\text{Co}_{0.8}\text{Bi}_{0.2}\text{O}_{2.87}$, which is having substitutions at both A- and B-sites. X-ray diffraction results revealed that the catalyst is single-phase and cubic in structure. The substitution of Bi for Co enhanced the catalytic activity of the perovskite-type oxides significantly. Over the Bi-incorporated catalyst, at equal space velocities and with the rise in CO/O_2 molar ratio, the temperature for 100% CO conversion shifted to a higher range; at a typical space velocity

of 30000 h^{-1} and a CO/O_2 molar ratio of 0.67/1.00, 100% CO conversion was observed at 250°C . Over $\text{La}_{0.8}\text{Ba}_{0.2}\text{Co}_{0.8}\text{Bi}_{0.2}\text{O}_{2.87}$, at equal CO/O_2 molar ratio, the temperature for 100% CO conversion decreased with a drop in space velocity; the lowest being 190°C at a space velocity of 5000 h^{-1}

Zhang *et al* (2002) investigated a series of Ce substituted La-Mn perovskite catalysts by co-precipitation method. The composition, bulk structure and surface properties were established using elemental analysis, XRD and XPS. They observed that Ce is not totally incorporated in the perovskite lattice. For a high degree of substitution an excess Ce form a separate CeO_2 phase. Simultaneously, an increase in the atomic $\text{Mn}^{4+}/\text{Mn}^{3+}$ ratio and a decreasing surface oxygen concentration were observed by them. They suggested that cation vacancies are created at A (La) sites, resulting in the formation of unsaturated Mn (B) site ions on the surface.

The catalytic activity of $\text{La}_{1-x}\text{Ce}_x\text{MnO}_3$ systematically changes as a function of the degree of Ce substitution. Among the catalysts prepared the highest activity being demonstrated by $\text{La}_{0.8}\text{Ce}_{0.2}\text{MnO}_3$.

Cimino *et al* (2003) studied the structural, redox and catalytic deep oxidation properties of $\text{LaAl}_{1-x}\text{Mn}_x\text{O}_3$ ($x = 0.0, 0.05, 0.1, 0.2, 0.4, 0.6, 0.8, 1.0$) solid solutions prepared by the citrate method and calcined at 1073K . Redox properties and the content of Mn^{4+} were derived from temperature programmed reduction (TPR) with H_2 . Two reduction steps are observed by TPR for pure LaMnO_3 , the first attributed to the reduction of Mn^{4+} to Mn^{3+} and the second due to complete reduction of Mn^{3+} to Mn^{2+} . The presence of Al in the $\text{LaAl}_{1-x}\text{Mn}_x\text{O}_3$ solid solutions produces a strong promoting effect on the $\text{Mn}^{4+} \rightarrow \text{Mn}^{3+}$ reducibility and inhibits the further reduction to Mn^{2+} . For CO oxidation all Mn-containing perovskites are much more active than LaAlO_3 , so pointing to the essential role of the transition metal ion in developing highly active catalysts. Partial dilution with Al appears to enhance the specific activity of Mn sites for methane combustion.

Dai *et al* (2003) prepared the highly active perovskite-type oxide $\text{La}_{0.6}\text{Sr}_{0.4}\text{Co}_{0.8}\text{Bi}_{0.2}\text{O}_{2.80}$ catalyst for CO Low-temperature oxidation. They characterized the material by means of XRD, TPR and BET. The catalytic activity was evaluated (0.2ml catalyst) at atmospheric pressure in a fixed bed quartz micro-reactor (i.d.=4mm).

The total flow rate of reaction mixtures CO/O₂/He was 100ml/min, with space velocity being 30,000h⁻¹. 100% CO conversion was achieved at 160°C for CO/O₂=0.67/1.00

2.3 HC OXIDATION

2.3.1 Simple perovskite catalysts

Teraoka *et al* (1984) compared the reduction behavior of Co₃O₄ and LaCoO₃ in the flow of a C₃H₄ (10vol %) /He mixture at 350°C. LaCoO₃ was found more resistant to reduction than Co₃O₄. Co₃O₄ was converted into CoO while with LaCoO₃ its crystal structure remained unchanged. This indicates that the Co³⁺ state is strongly stabilized in the perovskite matrix.

Seiyama *et al* (1985) compared the catalytic activity of several perovskites for the complete oxidation of propene with those of the corresponding constituent metal oxide (BO_n). It was seen that some oxides, such as, LaCoO₃ and LaFeO₃ show a positive effect where as some others a negative one. It has been shown that ABO₃ type perovskites have almost the same activities as their component oxides BO_n. This is rather surprising because in some oxides pair like LaNiO₃-NiO the normal valence of B cation changes with the formation of perovskite structure. Thus the activity of ABO₃ type perovskite is determined almost exclusively by the nature of component oxide BO_n; high activity is attained with perovskite of Mn and Co. The importance of the nature of B-site cations on ABO₃ has been pointed out by many researchers. However, it is remarked that the formation of a perovskite structure can still influence the catalytic activity to some extent by changes in the electronic and chemical state of B cations.

2.3.2 Substituted perovskite catalysts

Nakamura *et al* (1980) investigated the correlation between the oxidation activities with the surface concentration of B cations. For propane oxidation the effect of calcination temperature on the specific catalytic activity of La_{1-x}Sr_xCoO₃(x=0, 0.2) was seen. Although LaCoO₃ remained at almost the same activity level, La_{0.8}Sr_{0.2}CoO₃ followed a unique profile with a maximum at 850°C may be due to incomplete formation of the perovskite structure, while the loss of activity above 850°C was attributed to a change in surface composition, i.e., surface enrichment of A-site cations, especially Sr.

Fujii *et al* (1987) have shown the trend of catalytic activity of $\text{La}_{1-x}\text{Sr}_x\text{CoO}_3$ ($x=0, 0.2$) supported on various oxides. The catalysts were prepared by impregnating carrier oxide with aqueous solutions of mixtures of La, Co or Sr acetates. When the catalytic oxidation of propane was carried out over these supported catalysts, the rate varied greatly with the kind of oxide carrier. Most oxides loaded with $\text{La}_{0.8}\text{Sr}_{0.2}\text{CoO}_3$ showed very low activities, but high catalytic activity exceeding that of bulk $\text{La}_{0.8}\text{Sr}_{0.2}\text{CoO}_3$ was obtained when ZrO_2 or CeO_2 was used as support. When Al_2O_3 and SiO_2 were used as supports, the formation of CoAl_2O_4 and Co_2SiO_4 were observed, respectively. These reactions may be the reason why these catalysts showed very low activities. Zirconia supported perovskites showed high activity due to high dispersion of the catalyst on ZrO_2 .

Yamazoe *et al* (1990) presented the catalytic activity of Co-, Fe- and Mn-perovskites for the complete oxidation of propane as a function of Sr^{2+} substitution (x) for La^{3+} or Gd^{3+} . In all cases, activity changes significantly with x . Co- and Fe-systems show a steep activity maximum around $x=0.1-0.2$, while with a Mn-system a modest maximum at $x=0.6$ is reached. The optimum value of x , giving the highest activity in each system, depends on the reactant to be oxidized. In $\text{La}_{1-x}\text{Sr}_x\text{CoO}_3$, for example, the optimum x value is 0.2 for propane oxidation, 0.4 for n-butane oxidation and 0.1-0.6 for CO oxidation. It is found that Co- and Fe-perovskites tend to be optimized at smaller x value (0.1-0.4) than Mn-perovskites (0.6-0.8). It was further reported that the optimum value for $\text{La}_{1-x}\text{Ce}_x\text{CoO}_3$ depends on the calcination temperature used in the preparation. Two explanations were proposed for the activity variation with Sr substitution. The first one assumes that, as x increases, the amount of active oxygen increases while its specific reactivity decreases. The catalytic activity as determined by balancing these two factors becomes maximum eventually at an intermediate value of x . In the second explanation the assumption was made that an increase in x brings about an increase in reducibility (or oxidizing power) but a decrease in re-oxidation ability. A maximum activity at a certain value of x would thus be attained for which the redox cycle proceed most readily. In marked contrast, Mn-perovskites almost always catalyze the suprafacial reactions. This indicates that Mn-perovskites have little oxide ions for mobilizing lattice oxygen. Oxygen

is activated (adsorbed) at the surface catalytic sites to participate in the catalysis. The catalytic activity of $\text{La}_{1-x}\text{Sr}_x\text{MnO}_3$ thus varies as the amount of adsorbed oxygen varies.

Kwang *et al* (2001) investigated $\text{La}_{0.66}\text{Sr}_{0.34}\text{Ni}_{0.3}\text{Co}_{0.7}\text{O}_3$ perovskite, which is an excellent catalyst for the catalytic combustion of propane. They presented kinetics of a complete propane oxidation over $\text{La}_{0.66}\text{Sr}_{0.34}\text{Ni}_{0.3}\text{Co}_{0.7}\text{O}_3$ studied at a steady state in a plug-flow reactor. The experimental data were obtained for 0.5 g catalyst at temperatures between 473 and 613 K, with propane concentration varied from 0.58 to 4.76 vol.% oxygen between 7.5 and 98 vol. %, and flow rate between 100 and 400 ml/min. The $\text{La}_{0.66}\text{Sr}_{0.34}\text{Ni}_{0.3}\text{Co}_{0.7}\text{O}_3$ catalyst, prepared with high specific surface area of $15\text{m}^2/\text{g}$, shows again an excellent stable activity which competes favorably with that of noble metals. Several kinetic models have been tested. Best fit was obtained with the Mars–van Krevelen kinetic model. Nevertheless, the complete set of obtained data can also be fitted adequately by a simple power law model with 0.5 order in propane and 0.3 order in oxygen and apparent activation energy of 71 kJ/mol. Both water and carbon dioxide added to the feed have slight inhibiting effect, which was taken into account in a final extended Mars–van Krevelen kinetic model

Florina *et al* (2002) studied the catalytic activity of $\text{La}_{0.8}\text{A}_{0.2}\text{MnO}_3$ (A = Sr, Ba, K, Cs) and $\text{LaMn}_{0.8}\text{B}_{0.2}\text{O}_3$ (B = Ni, Zn, Cu) catalysts for the oxidation of lean mixtures of hydrogen or propene in the temperature range of 200–450°C (hydrogen) and 150–550°C (propene), respectively. The catalytic features were correlated with the redox behavior of the oxides as revealed by temperature-programmed reduction (TPR) experiments. The highest activity for hydrogen oxidation was found over strontium, barium and copper substituted manganites, whereas in the case of propene oxidation the copper substituted perovskite showed substantially lower activity, which was assigned to the stronger bonding of the produced carbon dioxide to the copper centers. The results are discussed with regard to the concepts of suprafacial and intrafacial catalysis. Apart from the temperature control, the occurrence of one or another of the two mechanisms is imposed by the nature of the substituted cation.

Lucio *et al* (2002) studied the advantages and disadvantages of the catalysts so far employed or proposed for the low temperature catalytic combustion of hydrocarbons, in both static and mobile energy production devices. Furthermore, a $\text{La}_{0.9}\text{Ce}_{0.1}\text{CoO}_{3\pm\delta}$

perovskite has been prepared by a recently proposed new flame-hydrolysis (FH) method. This proved a high surface area, thermally highly resistant catalyst. The partial substitution of Ce for La in such a cobaltite led to a relatively low superficial activity, but to a high bulk oxygen mobility, leading to high intrafacial activity for the catalytic flameless combustion of methane. The best operating conditions have been also found, for supporting the so prepared active phase, by dip-coating of a cordieritic honeycomb support, after deposition of an alumina primer. A very active and durable catalyst was so obtained, useful for practical application in the environmentally friendly low temperature combustion of methane.

Oliva *et al* (2006) prepared a few $\text{La}_{1-x}\text{Ce}_x\text{CoO}_3$ ($x = 0; 0.1$) catalysts using the traditional sol-gel (SG) or by flame pyrolysis (FP) procedures. These catalysts have been analysed by XRD, EPR and BET. The catalytic activity was measured by loading 0.2 g of catalyst, diluted with 1.3 g of quartz powder of the same particle size (60–100 mesh) in a continuous tubular micro reactor, to which a mixture of $20 \text{ cm}^3 \text{ min}^{-1}$ of a 1 vol% CH_4 in N_2 + $20 \text{ cm}^3 \text{ min}^{-1}$ of air was fed, while increasing temperature by 2Kmin^{-1} up to 873 K. among the catalysts prepared, $\text{La}_{0.9}\text{Ce}_{0.1}\text{CoO}_3$ (fresh FP1) showing higher activity for CFC of methane.

2.4 OXIDATION OF CO AND HC

2.4.1 Simple perovskite catalysts

Johnson *et al* (1990) synthesized zinc ferrite by co-precipitation and ceramic techniques and dispersed them on monolithic ceramic support and evaluated their performance for the oxidation of CO and HC Conversion efficiencies of 67% and 65%, respectively, have been achieved for CO and HC. Rates of oxidation for CO and propane showed a linear dependence upon the surface area of LaCoO_3 from room temperature to 600°C (Barnard *et al.*, (1990))

Jovanovic *et al* (1991) synthesized single phase perovskites, as LaCoO_3 , LaCrO_3 , $\text{LaCo}_{0.5}\text{Cr}_{0.5}\text{O}_3$, $\text{La}_{0.7}\text{Sr}_{0.3}\text{CrO}_3$ and $\text{La}_{0.7}\text{Sr}_{0.3}\text{Cr}_{0.5}\text{Ru}_{0.05}\text{O}_3$, and measured the three-way activity and sulfur tolerance in a pulse-flame catalyst testing system in a wide range of redox potential. Comparison of activities indicates that perovskite with ruthenium ion has the best redox behaviour in the redox potential interval $0.75 < R < 1.40$. On the basis of

experimental data, the sulfur resistant matrix $\text{La}_{0.7}\text{Sr}_{0.3}\text{CrO}_3$ was synthesized and the highly active sulfur resistant ruthenium perovskite catalyst was prepared.

Yao *et al* (1996) investigated cordierite honeycomb catalysts supported on rare earth (RE) transition metal oxides for removing simultaneously three major pollutants, carbon monoxide (CO), hydrocarbon (HC) and nitrogen oxides (NO_x), in automobile emission. The results indicate that the catalyst has improved three-way performance (TWP).

2.4.2 Substituted perovskite catalysts

Bradow *et al* (1995) used perovskite type catalysts $\text{La}_y\text{Sr}_{1-y}\text{Ru}_x\text{Cr}_{1-x}\text{O}_3$ ($y=0.7; 0.025 < x < 0.1$), which were synthesized by the ceramic method, in activity measurements in the simultaneous conversion of CO, HC and NO_x in the pulse flame catalyst testing (PFCT) system and synthetic dry gas mixtures. In the presence of water vapor, in the reaction mixture (PFCT system), an unusually high level of CO oxidation and a higher concentration of H_2 detected in the outlet reactor gases, compared to the inlet reactor gases, can be ascribed to a water gas shift reaction. The generated hydrogen, present on the catalyst surface in its dissociated form, could be responsible for the higher NO_x conversion under net oxidizing (lean) conditions, which favors ruthenium synthesized catalysts as three way auto exhaust catalysts.

Guihaume *et al* (1996) investigated a series of palladium substituted La_2CuO_4 , corresponding to the formula $\text{La}_2\text{Cu}_{1-x}\text{Pd}_x\text{O}_4$ ($x=0-0.2$) were prepared by metal nitrate decomposition in a polyacrylamide gel. The partial substitution of copper for palladium allows a strong improvement of the three way catalytic activity, in particular for NO reduction. The light off temperatures for the conversions of CO, NO and C_3H_6 decreased markedly when increasing the palladium content, the catalytic activity of $\text{La}_2\text{Cu}_{0.9}\text{Pd}_{0.1}\text{O}_4$ and $\text{La}_2\text{Cu}_{0.8}\text{Pd}_{0.2}\text{O}_4$ being comparable to that of a Pt-Rh/ CeO_2 - Al_2O_3 catalyst for NO reduction, and higher for CO and C_3H_6 oxidation.

Sharma *et al* (1998) tested $\text{La}_{0.85}\text{Ce}_{0.15}\text{CoO}_3$ catalyst for the oxidation of CO and C_3H_6 . The catalysts were characterized by using XRD, TGA, SEM and BET analysis. The catalytic activity studies were performed in a capillary fixed bed tubular reactor (i.d=2.46mm). The effluent gases were analyzed using gas chromatograph. 100%

conversion of CO is obtained at 200°C on La_{0.85}Ce_{0.15}CoO₃ catalyst, calcined at 960°C and 100% conversion of C₃H₆ obtained at 375°C.

Dahl *et al* (1998) studied the catalytic activity of La_{1-x}Sr_xGa_{1-y}Cu_yRu_yO₃ (x= 0, 0.2; y=0, .35) on the oxidation of CO and C₃H₆. The samples were characterized by X-ray diffraction, scanning electron microscope and analytical transmission electron microscopy studies. Selected sample were subjected to catalytic tests with respect to oxidation of CO and C₃H₆ and reduction of NO under rich and lean conditions, respectively. The replacement of some Ga by Cu and Ru ions improved the catalytic activity for the oxidation of NO under rich conditions. Whereas under lean conditions, no activity for the reduction of No was observed. The light-off temperatures recorded under rich conditions for the oxidation of Co and C₃H₆ and reduction of NO for the La_{0.8}Sr_{0.2}Ga_{0.8}Cu_{0.1}Ru_{0.1}O₃ samples prepared insitu, T₅₀=374, 357 and 461°C, respectively, were 50-100°C lower than for the exsitu prepared sample.

Song *et al* (1999) studied the activities of La_{1-x}M_xMnO₃ (M= Ag, Sr, Ce, La) catalysts on CH₄ and CO oxidation. Various La_{1-x}M_xMnO₃ (M= Ag, Sr, Ce, La) catalysts were prepared by co-precipitation and spray decomposition method. The spray decomposition method produced perovskites of a high surface area of over 10m²/g. the catalytic activities for CH₄ and CO oxidation have been studied on a series of catalysts La_{1-x}M_xMnO₃.the perovskite type oxide La_{0.7}Ag_{0.3}MnO₃ shows the highest catalytic activity: the complete conversion of CO and CH₄ at 370 and 825K respectively.

He *et al* (2001) investigated the perovskite-type oxides La_{1-x}Sr_xMO₃ (M = Co_{0.77}Bi_{0.20}Pd_{0.03}) for three-way catalytic performance. The catalysts were characterized by means of temperature-programmed desorption (TPD), temperature-programmed reduction (TPR), X-ray diffraction (XRD), and X-ray photoelectron spectroscopy (XPS). The catalysts exhibited good activity in CO elimination: La_{0.8}Sr_{0.2}MO₃ showed ca. 100% CO conversion at 160°C, 60 000 h⁻¹, and λ = 1.00. Under similar reaction conditions, the activity for C₃H₆ elimination decreased in the order of La_{0.2}Sr_{0.8}MO₃ > La_{0.8}Sr_{0.2}MO₃ > La_{0.4}Sr_{0.6}MO₃ > La_{0.6}Sr_{0.4}MO₃ > LaMO₃, while the activity for NO elimination decreased in the order of La_{0.8}Sr_{0.2}MO₃ > La_{0.2}Sr_{0.8}MO₃ > La_{0.4}Sr_{0.6}MO₃ > La_{0.6}Sr_{0.4}MO₃ > LaMO₃. With x < 0.6, La_{1-x}Sr_xMO₃ were single-phase and hexagonal in structure; at x = 0.6 and 0.8, they were cubic and there was a trace amount of the La₂O₃ phase. The results of

TPD, TPR, and XPS studies revealed the coexistence of over-stoichiometric oxygen vacancies in $\text{La}_{0.8}\text{Sr}_{0.2}\text{MO}_3$, a criterion for good three-way catalytic performance.

Tanaka *et al* (2003) used $\text{La}_{0.9}\text{Ce}_{0.1}\text{Co}_{1-x}\text{Fe}_x\text{O}_3$ catalyst for oxidation of CO, HC and NO_x . One of the most important issues of automotive catalysts is the endurance of fluctuations between reductive and oxidative (redox) atmospheres at high temperatures exceeding 1173K. The catalytic activity and structural stability of $\text{La}_{0.9}\text{Ce}_{0.1}\text{Co}_{1-x}\text{Fe}_x\text{O}_3$ perovskite catalysts ($x = 0, 0.2, 0.4, 0.6, 0.8$ and 1.0), both in powder and monolithic forms, were investigated after aging treatments in real and simulated “model” automotive exhaust gases. For powder catalysts before and after treatment both in the redox model gas and in air, the activity for oxidation of propane was evaluated and correlated with the crystal structure. For monolithic catalysts, the activities for reduction of NO, oxidations of CO and hydrocarbons (HC) were evaluated before and after aging in the flow of an engine exhaust gas at 1173 K. With increasing Co in $\text{La}_{0.9}\text{Ce}_{0.1}\text{Co}_{1-x}\text{Fe}_x\text{O}_3$ perovskite catalysts, the catalytic activity increased and the structural stability decreased. $\text{La}_{0.9}\text{Ce}_{0.1}\text{Co}_{0.4}\text{Fe}_{0.6}\text{O}_3$ indicated the best balance of activity and durability in the automotive exhaust gas at high temperatures. When the fraction of Co exceeded 0.6, the activity diminished due to the structural transformation from perovskite to K_2NiF_4 -type layered structure. These observations, in general, corresponded to the results obtained for Pd-promoted perovskite monolithic catalysts. Specifically Fe at B-site gave the durability, and Co as well as Pd improved the activity of perovskite catalysts applied to automotive emissions control.

Yang *et al* (2004) invented the perovskite like $\text{La}_{2-x}\text{Sr}_x\text{CoO}_{4\pm\lambda}$ mixed oxides of K_2NiF_4 structure by using the polyglycol gel method and used successfully for Co and C_3H_6 oxidation. These samples were characterized by using the XRD, IR, TEM, BET, TPD and iodometry methods; and the effect of coefficient x on their structure and catalytic activities of these samples were studied for the first time. The results shows that La_2CoO_4 has orthorhombic K_2NiF_4 type structure, when La^{3+} is substituted by Sr^{2+} , whose ionic radius is larger than that of La^{3+} , the structure factor increases, and this leads to the structure changes from orthorhombic system to tetragonal system. In addition, these catalysts possess different catalytic activity towards the oxidation of CO and C_3H_6 , this is

explained in terms of their structure: mobile lattice oxygen, content of Co^{3+} particle sizes and BET surfaces

Uenishi *et al* (2005) studied the three way catalytic activity of LaFePdO_x . In order to elucidate the activity of LaFePdO_x -based automobile three-way catalysts at low-temperatures, the oxygen release capacity (ORC) and oxygen storage capacity (OSC) of LaFePdO_x were measured by means of thermogravimetry (TG) in a hydrogen-containing atmosphere at 200–400 $^{\circ}\text{C}$ and NO reduction activity was examined at 400 $^{\circ}\text{C}$ by an NO-pulse technique. The catalyst weight-loss in reduction was attributed to oxygen release, leading to the formation of metallic Pd^0 . About 40% of Pd^{3+} in $\text{LaFe}_{0.95}\text{Pd}_{0.05}\text{O}_3$ was converted into Pd^0 at 200 $^{\circ}\text{C}$ and about 90% at 400 $^{\circ}\text{C}$. ORC and OSC as observed for the LaFePdO_x catalysts were found to be comparable to results seen when adding Ce-based oxides as an OSC material in a commercial catalytic converter. The reducing capability of Pd for NO reduction demonstrated by the reduced LaFePdO_x catalysts can probably be attributed to the very fine dispersion of Pd^0 species segregated from $\text{LaFe}_{0.95}\text{Pd}_{0.05}\text{O}_3$ perovskite. The Pd^0 species segregated from LaFePdO_x by reduction was assessed to be metallic Pd^0 particles with diameters smaller than 2 nm. Highly dispersed Pd^0 particles on the LaFePdO_x catalyst were found to act as “breathing active sites” that combined high catalytic activity with OSC/ORC performance.

Yang *et al* (2005) prepared the perovskite-like LaSrCoO_4 mixed oxides using the gelatin, polyglycol gel and polyacrylamide gel methods and were used successfully for the CO and C_3H_8 oxidation. These samples were characterized by using the XRD, TEM, BET and TPD methods. The effects of preparation methods on the structure and performance of LaSrCoO_4 were studied. The catalytic activity of LaSrCoO_4 prepared by polyacrylamide gel method is the best among all the samples.

2.5 CHARACTERISTICS OF PEROVSKITES

2.5.1 Surface composition of perovskites

Perovskites are assumed to have well-defined structures. However, their surface compositions have been reported to differ significantly in some cases from the bulk, depending on the conditions in which they are prepared and the bulk composition. The

surface often tends to be poor in catalytically active B-site cations and Nakamura et al. (1980) have even correlated the oxidation activity with the surface concentration of B cations. Although LaCoO_3 remained at almost the same activity level, $\text{La}_{0.8}\text{Sr}_{0.2}\text{CoO}_3$ followed a unique activity profile with a maximum at 850°C . This may be due to incomplete formation of the perovskite structure, while the loss of activity above 850°C is attributed to a change in surface composition, i.e., surface enrichment of A-site cations, especially Sr. It was reported by Teraoka *et al* (1988) that even the surface of calcined $\text{La}_{1-x}\text{Sr}_x\text{CoO}_3$ was subjected to change in composition during the subsequent evacuation-oxidation treatments at temperatures above 500°C , leading to the reduction of catalytic properties. All these results suggest the versatile nature of the perovskites with well-defined surface with respect to structure and composition.

2.5.2 Thermal stability

The main advantage of perovskites is the improved resistance against reduction and heat. Lauder *et al* (1975) reported that the catalytic activities of $\text{La}_{0.8}\text{Sr}_{0.2}\text{Co}_{0.9}\text{Pt}_{0.1}\text{O}_3$ and $\text{La}_{0.8}\text{Sr}_{0.2}\text{Co}_{0.9}\text{Ru}_{0.1}\text{O}_3$ for CO oxidation did not change after the treatment in air at 900°C for 300 h.

Tabata *et al* (1986) examined the thermal stability of $\text{La}_{0.9}\text{Ce}_{0.1}\text{CoO}_3$ (prepared by calcination at 850°C) and a commercial Pt catalyst (0.5 wt% Pt/ Al_2O_3). After the catalyst was heated in air at 800°C for various periods in a mantle heater, the catalytic activities were measured for the oxidation of CO at 600°C . As shown in Fig. 2.1, the catalytic activity of $\text{La}_{0.9}\text{Ce}_{0.1}\text{CoO}_3$ did not change at all even after 1000 h-life test, although the activity of the Pt catalyst dropped significantly [Matsumato et al., 1986].

2.5.3 Sulphur resistance

Thermal aging, SO_2 poisoning, and reaction of the active phase with the support are factors that are known to be important in the deactivation of solid catalysts. Noble metals are usually poisoned by lead, whereas base metal oxide catalysts are more susceptible to poisoning by sulfur. Indeed, the deactivation of oxides when used in oxidation or 'seduction has been attributed to a large extent to SO_2 .

Yao et al (1975) studied the effect of SO₂ on the catalytic activity of perovskites in relation to their potential as oxidation catalysts for automobile exhausts. Usually, base metal oxides are more resistant to lead than noble metal catalysts, but are more susceptible to poisoning by sulphur. The rate was severely reduced by the presence of few ppm of SO₂ below 500°C. However, in the case of La_{0.7}Pb_{0.3}MnO₃ prepared in Pt crucibles or doped with 100 ppm of Pt, an increase in activity was observed with a long time exposure to reaction mixture containing 10-30 ppm of SO₂.

Some perovskites were reported to be highly resistant to poisoning by lead compounds. In less resistant oxides, lead poisoning may be reduced or avoided by introducing element in position A of the structure. The addition of small amounts of Pt to lead perovskites results also in an improvement of their oxidation activity in the presence of SO₂. Thus **Yao (1975)** observed that the catalytic activity for C₂H₄ oxidation of La_{0.7}Pb_{0.3}MnO₃ containing 30ppm of Pt increased remarkably after admitting 0.1% SO₂ to the reacting mixture at 500°C. This high activity did not change on removal of SO₂ from gaseous phase

A similar SO induced effect in CO oxidation was reported by **Gallagher et al. (1975)** for the above mentioned perovskite doped with 570 ppm of Pt. This enhanced activity was accounted for by assuming that Pt was bonded to or covered by Pb, and SO₂ freed Pt through the formation of PbSO₄. Water favoured this process by increasing the diffusion of lead sulfate from the vicinity of Pt. Katz et al. (1975) also studied the resistance of La_{0.7}Pb_{0.3}MnO₃ to 0.1% SO₂. The activity for CO oxidation decreased less in comparison with Co₃O₄ and CuO. However, Pt/Al₂O₃ was more resistant, as there was no significant loss of activity after 24 h of exposure.

Minming et al (1983) observed that the SO₂ poisoning of La_{0.5}Sr_{0.5}MnO₃ for CO oxidation occurred through both a fast process and a slow process. These authors detected two adsorbed species of SO₂: -SO₂ and -OSO₂. On the basis of these facts they assumed that there were two different kinds of active centers, Mn- and MnO-. Sulfate formation was also detected. These results had shown that the poisoning effect of SO₂ on these perovskites occurred through the adsorption of this molecule on B sites or oxygen anions that were centers responsible for the catalytic action in these compounds. SO₂ may also

interact with cations in position A, but this process does not result in the deactivation of the catalyst.

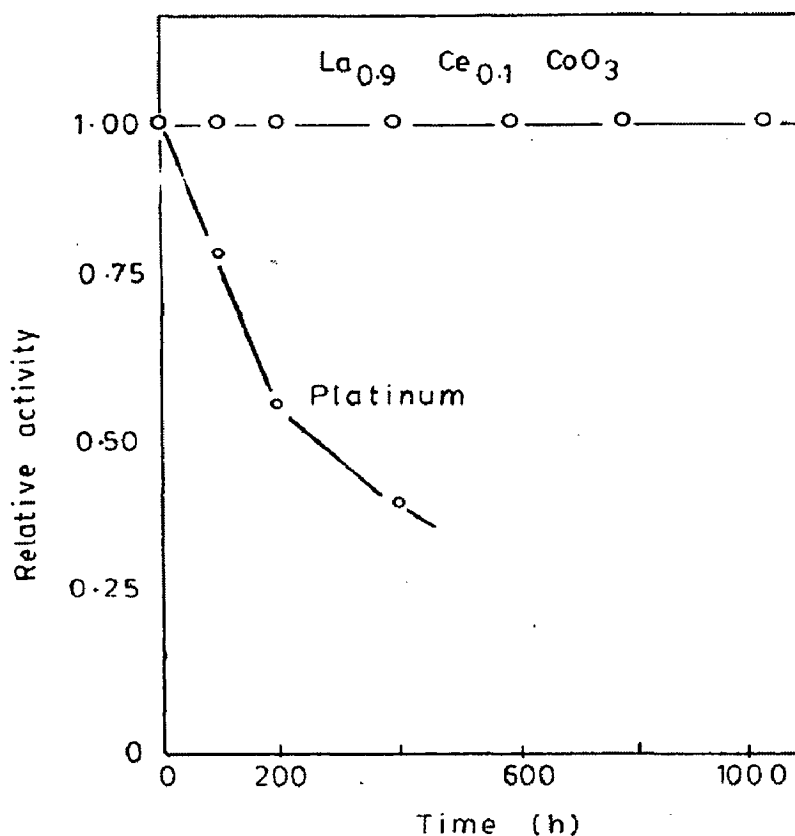


Fig. 2.1 Thermal stability of 0.5 Pt/Al₂O₃ and La_{0.9}Ce_{0.1}CoO₃ for propane oxidation at 600°C (Matsumoto *et al* 1986)

↑
p. 28

Although some progress has been attained in the preparation of highly active perovskites for CO and hydrocarbon oxidation and NO reduction by the incorporation of noble metals (Pt and Ru) into the structure, the problem of SO₂ poisoning remains basically unsolved. From the measurements of catalytic activity and reducibility on fresh and SO₂ poisoned perovskites, **Wan *et al* (1987)** concluded that a high mobility of the lattice oxygen and the ability to form weaker bonds with sulfur were essential factors for

improving the SO₂ resistance of perovskites in oxidation processes. For this to be achieved, further spectroscopic studies will be needed, in order to gain a better insight into the nature of the interactions of SO₂ with the surface of these compounds.

EXPERIMENTAL SETUP AND PROCEDURE

3.1 General

Having fixed the aims and objectives on the basis of literature review, we embarked upon an extensive research program on catalysts preparation, their characterization and their performance on carbon monoxide and propylene oxidation.

3.2 Preparation of $\text{La}_{1-x}\text{M}_x\text{Co}_{1-y}\text{Bi}_y\text{O}_{3\pm\delta}$ (M= Ag, Ce, Sr; x=0, 0.3; y=0, 0.2)

3.2.1 Co-precipitation method

3.2.1.1 Precipitation of metal ions

$\text{La}_{1-x}\text{M}_x\text{Co}_{1-y}\text{Bi}_y\text{O}_{3\pm\delta}$ (M= Ag, Ce, Sr; x=0, 0.3; y=0, 0.2) was prepared by co-precipitation of metal nitrates with the addition of ammonium hydroxide solution. The procedure was as follows: the required amount (depends on value of x and y) of nitrate salts of lanthanum, silver, cobalt and bismuth were dissolved in distilled water. The precipitate of salts was formed by the addition of aqueous solution of ammonium hydroxide rapidly at room temperature. The pH of the solution was maintained around 7-9, which ensured the co-precipitation of different metal ions.

3.2.1.2 Heat treatment of catalyst

The precipitate along with the supernatant solution was kept in an oven at 110°C for 15-16 hours for drying the precipitate by evaporating water. Subsequently step wise calcination was performed by heating the dried precipitate from 150°C to different terminal temperatures of 600°C, 700°C, 800°C in a step of 50°C. Calcination was done 24h at 600°C, 12h at 700°C and 5h at 800°C. The dried precipitate was first heated in a muffle furnace with increase in temperature at a rate of 10°C per minute from one temperature to the subsequent higher temperature. The calcination at 600°C was completed in 4 day-6h heating every day. At 700°C, it was completed in two days while at 800°C it was done in one day. After heating every day, the material was furnace

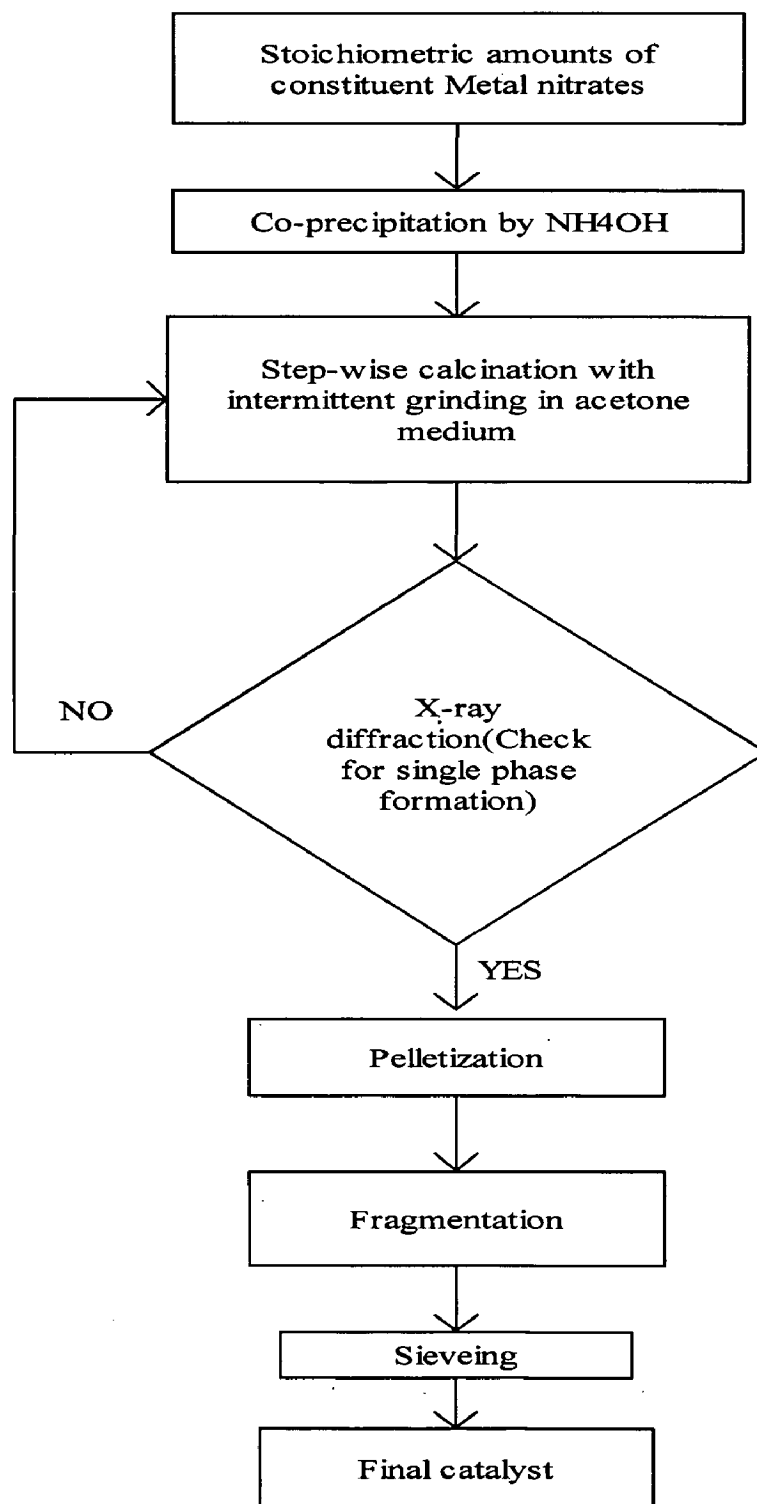
cooled, palletized and grounded in acetone with a pastel and mortar. The grounded material was further heated in the next day at the terminal temperature. Thus the calcined material at 600°C was grounded in-between four times; where as at 700°C, it was grounded in once in-between. The calcination at 800°C was completed without in-between grinding of the material. The calcined material was pelletized in the pellet machine at a pressure of 10 tonnes/cm². The pellets, so formed, were broken to the appropriate size and then heated up to 600°C for 5h. After the heat treatment, the catalyst particle were crushed and sieved. The fraction of particles in the size range of 250-600µm will be used in the reactor. The heat treatment cycle followed in the preparation of the catalyst is shown in table 3.1. Various stages during the synthesis of supported catalysts are shown in Fig.3.1. After screening the catalyst material were characterized by using XRD analysis, Scanning Electron Microscope (SEM) and Thermo Gravimetric Analysis (TGA).

Table 3.1 Calcination temperature and heating schedule

S.No	Temperature, °C	Duration, h
1	200	24
2	300	18
3	400	12
4	500	8
5	600	6
6	700	6
7	800	6

3.2.2 Dry mixing method

The preparation of the catalysts was done by mixing the stoichiometric amounts of nitrate salts of Lanthanum, Silver, Cobalt and Bismuth. The required amounts of La(NO₃)₃.6H₂O, Co(NO₃)₂.6H₂O, AgNO₃, Bi(NO₃)₃.5H₂O were taken and grinded into very fine powder in a pastel and mortar. After grinding the material was heat treated in an electric furnace.



3.1. Flow sheet for the preparation of catalyst by Co-precipitation method

The calcination of the catalyst was done at different terminal temperatures like 250°C, 500°C and 800°C. The catalyst was calcined for 8 h at 500°C and for 16h at 800°C. After calcining at each temperature, the material was furnace cooled and then grounded in acetone with a pastel and mortar. The grounded material was further heated the next day at the terminal temperature. After the heat treatment the catalyst material was characterized by using XRD, TGA and SEM analysis.

3.3 Catalyst Characterization

3.3.1 X-Ray diffraction (XRD) analysis

The determination of structure of $\text{La}_{0.7}\text{M}_{0.3}\text{Co}_{0.8}\text{Bi}_{0.2}\text{O}_{3\pm\delta}$ (M= Ag, Ce, Sr) catalyst was done by X-ray diffractometer (Philips PW 1140/90) in Institute Instrumentation Center (IIC), IITRoorkee by using Cu-K_α as a source and Ni as a filter. Goniometer speed was kept at 1°/min and chart speed was 1 cm/min. The range of scanning angle (2θ) was kept at 5-90°. During the analysis the goniometer was scanned over its angular range and a plot of 2θ against intensity was obtained. The intensity peaks indicate values of 2θ where Bragg's law $n\lambda=2d\sin \theta$ is fulfilled.

3.3.2 Scanning electron micrograph

To study surface structure and morphology of the catalysts scanning electron micrographs was obtained using a Philips SEM-501 microscope at the Institute Instrumentation Centre (IIC), IIT Roorkee. Depending on the clarity of the visible images the magnification and resolution values were selected.

3.3.4 Thermo gravimetric analysis

Thermo gravimetric analysis (TGA), differential thermal analysis (DTA) and derivative thermo gravimetric analysis (DTGA) were carried out for catalysts, in air by means of Stanton-Reel croft STA 781 thermal analysis system at IIC, IIT Roorkee. Specifications are shown in Table 3.5

Table 3.2 specifications for thermal analysis

Sample amount	10mg
Temperature range	Ambient to 100°C
Heating rate	10°C per minute
Reference material	Alumina
Furnace winding	Rhodium-Platinum
Sample holder	Pt crucible of dia.6 mm and height 4mm

3.4 EXPERIMENTAL SET-UP

The activity of the prepared catalysts was tested using an experimental apparatus. The schematic representation of the experimental set-up is shown in Fig. 3.2. The set-up consists of four sections:

1. Metering and mixing of feed gases
2. Reactor
3. Temperature control
4. Computer aided analysis and monitoring of the gases

3.4.1 Metering and mixing of feed gases

The source of feed gas was from two cylinders, one containing zero air having 21% O₂ and balance nitrogen, while the other cylinder contained a mixture of gases having a specific composition of 2% CO, 0.25% propylene and balance nitrogen. The flows of both the gaseous streams were controlled by precision valves at a particular pressure with the help of pressure gauges (0-4 kg/cm²). The gases on the downstream side of the valves then entered through water bubblers before entering into the reactor. The flow measurement was done with an on-line soap film gas flow meter.

3.4.2 Reactor

The reactor used was a quartz glass tube with inner diameter of 4 mm, outer diameter 6 mm and length of 315 mm. The reactor was placed horizontally inside a tubular, electrically heated furnace. The temperature was controlled by a P.I.D. temperature controller. The reactor temperature was measured by a ceramic sheathed chromel-alumel thermocouple placed co-axially along the reactor. The reactor has three

zones pre-heating, reaction and the post heating zones. The inlet or preheating zone is 150 mm long and is packed with glass wool. The reaction zone is 20 mm long and is packed with catalyst particles. The post heating zone is 145 mm long and its initial 10 mm portion is packed with glass wool mainly for the purpose of supporting the catalyst. Reactor outlet to the gas chromatograph inlet was connected by a minimum possible length of tube to minimize the time required for effluent gases to reach the GC inlet.

3.4.3 Analytical system

The analytical system is governed by a personal computer, interfaced with gas chromatograph. A set of software programs and subroutines permit us to collect, store, and process the analytical data in many different ways. Quantitative analysis of the chromatogram was obtained by electronic integration of the peak areas using the computing integrator attached with the output signals of the GC. Response factors were obtained, by integration of chromatograms for calibration gases.

3.5 Experimental Procedure

Catalytic activity tests were conducted in the reactor assembly equipped with fixed catalyst bed. The catalyst particles were packed in the mid length portion of the reactor, The catalyst was supported on both sides by glass wool, which serve as pre- and post- heating zones for the reacting gases and ensure the uniformity of flow of gases in the reactor. 0.7 to 0.9g of fresh catalyst of particle size 250-600mm was charged in each run in order to occupy a 4 cm length in the reactor tube. Catalyst volume in all the tests was, thus, kept constant at 0.502 cm³. The activity tests were performed at temperatures ranging from 100- 300°C in 25°C/ 50°C interval. The temperature was maintained to ± 1% accuracy. Space velocity during the tests was kept at 13850 h⁻¹.

The flow rate and the composition of feed gas were adjusted by controlling the flow rate of individual gases by non-return precision valves, which was calibrated by the soap film gas flow meter.

Gaseous mixture having composition (2% CO + 0.25% Propylene + 3-4 %O₂+ 6-8% H₂O and balance N₂) was used as feed gas in most of the runs. The flow rate from CO cylinder was approximately three times the flow rate from O₂ cylinder and the total flow

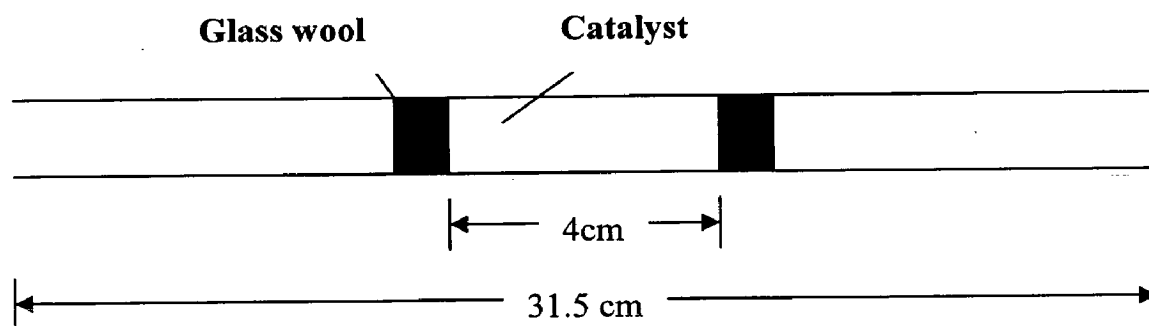
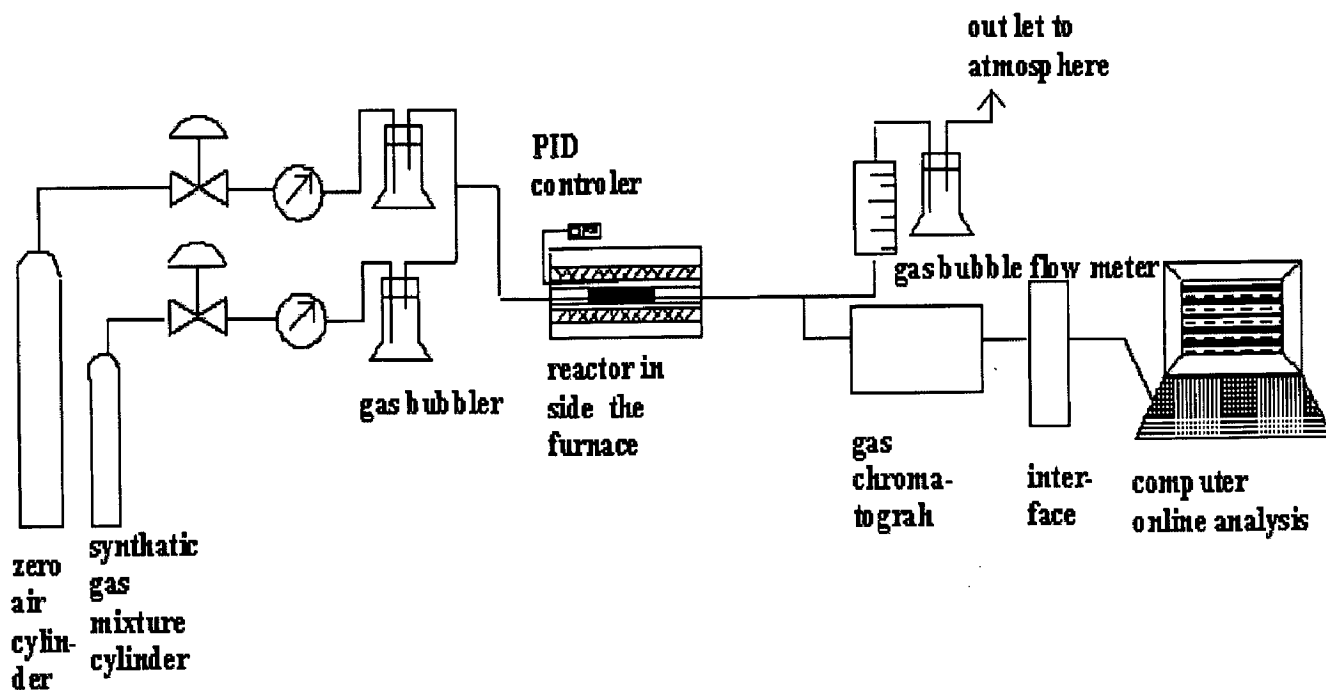


Fig3.2: The schematic representation of the experimental set-up

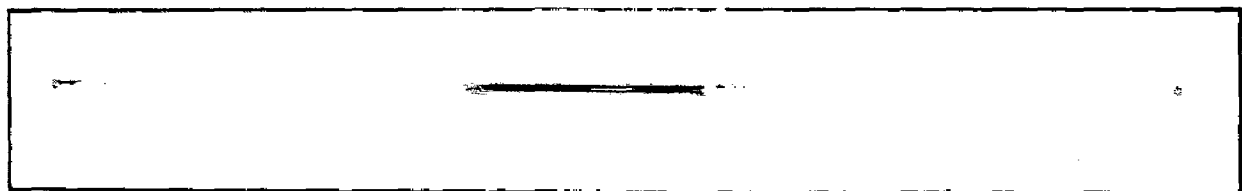
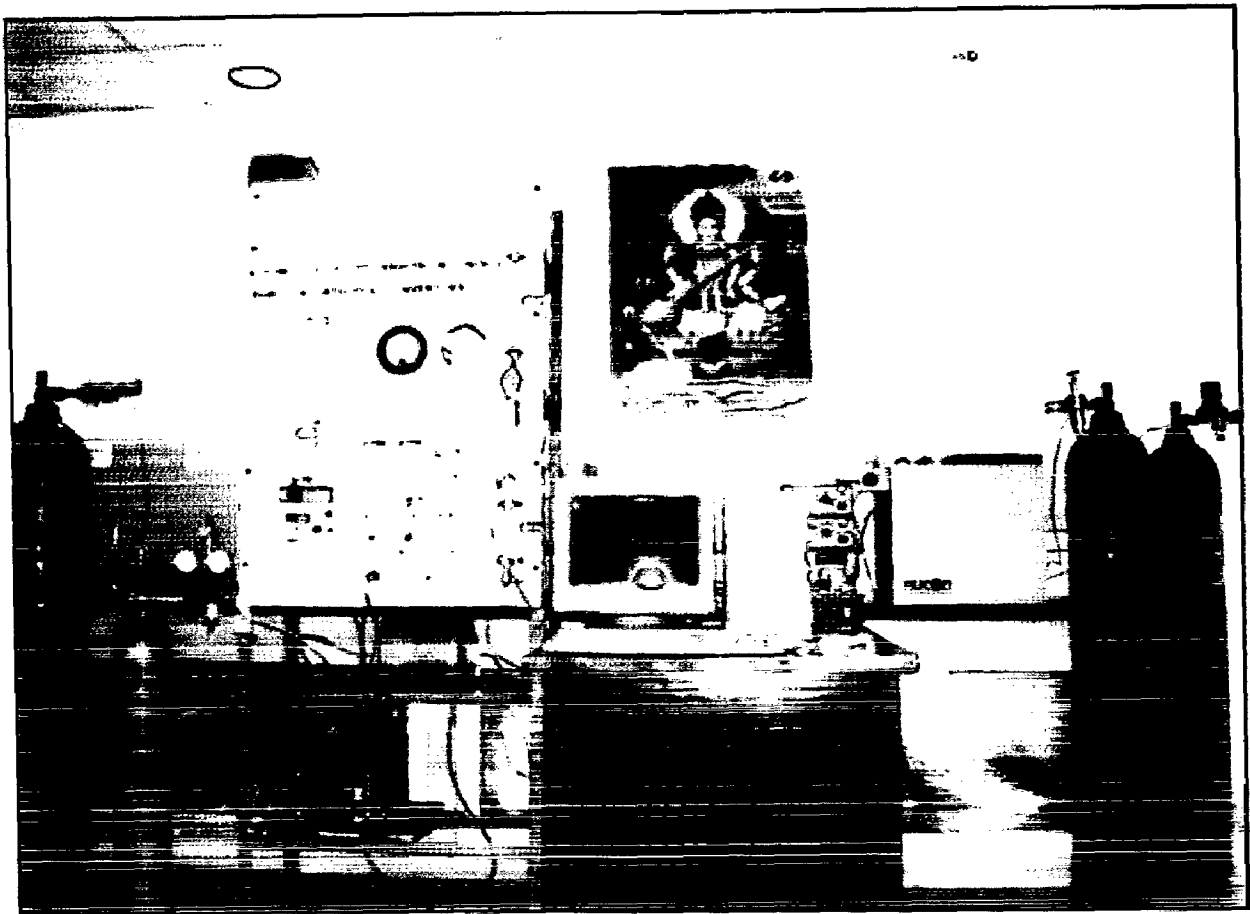


Fig 3.3: Photograph of Experimental set-up and fixed bed micro reactor

rate of the mixture was 30 ml/min. The incorporation of water bubblers in both feed lines blocked the cross flow of the gases as well as ensured the presence of water vapor in the reactant mixture (around 6-8 % by volume) which is desirable to simulate the actual gas.

3.6 Gas Chromatographic Analysis

For the analysis of the reactants and the products, a NUCON-5700 dual column gas chromatograph equipped with 2 m x 3 mm diameter stainless steel column packed with molecular sieve 5A° (80-100 mesh) and 2 m x 3 mm diameter stainless steel column packed with PorapakQ (80-100 mesh) were used. Thermal conductivity detector (TCD) was used in the analysis of the gases. Hydrogen of grade-I purity was used as the carrier gas with a flow rate of 25 ml/min in both the columns. For the determination of the area of various peaks and the concentration of the reactants and the products, an integrator software (NUCON- ORACLE2) was used.

3.6.1 CO analysis

For the detection of CO as well as O₂ in the feed and the product, molecular sieve 5 A° column in the G.C. was fitted to the on-line sampling valve and the test conditions were set as given in Table 3.2. Feeding of reactant and the reactor product gases to the gas chromatograph was done through a six-port valve. The simultaneous analysis of CO and O₂ enabled us to check and maintain the input feed stream composition as constant in each run. The sequence of the eluted gases was oxygen, nitrogen and carbon monoxide.

3.6.2 Propylene analysis

For Propylene detection, Porapak-Q column was fitted to the on line sampling valve. Porapak-Q column facilitated simultaneous analysis of C₃H₆, CO₂, and H₂O in the feed gas as well as in the reactor product stream. Test conditions for propylene are given in Table 3.3. The sequence of the eluted gases was be (nitrogen + oxygen + carbon monoxide), carbon dioxide, water and propylene.

Table 3.3 GC conditions for CO analysis

S.NO.	Item	Setting
1.	Detector	TCD
2.	Injector temperature	90°C
3.	Detector temperature	90°C
4.	Oven temperature	60°C
5.	Carrier gas	Hydrogen
6.	Carrier gas flow rate	30 ml/min
7.	Carrier gas pressure	1.2 kg/cm ²
8.	Gas chromatographic column	Stainless steel 2 mm x 1.82 m Molecular-sieve 5A° (60-80mesh)
9.	Attenuation	4
10.	Sample injection loop fitted to GC	1 ml on line loop

Table 3.4: GC conditions for C₃H₆ analysis

S.NO.	Item	Setting
1.	Detector	TCD
2.	Injector temperature	110°C
3.	Detector temperature	110°C
4.	Oven temperature	80°C
5.	Carrier gas	Hydrogen
6.	Carrier gas flow rate	30 ml/min
7.	Carrier gas pressure	0.8 kg/cm ²
8.	Gas chromatographic column	Stainless steel 2 mm x 1.82 m Porapak-Q (80-100mesh)
9.	Attenuation	4
10.	Sample injection loop fitted to GC	2 ml on line loop

RESULTS AND DISCUSSION

4.1 RESULTS

The characterisation of laboratory synthesized perovskite catalysts and their activity results on the oxidation of CO on these catalysts have been presented in this chapter. Characterization studies include XRD, TGA and SEM.

4.1.1 CHARACTERIZATION OF $\text{La}_{1-x}\text{M}_x\text{Co}_{1-y}\text{Bi}_y\text{O}_{3\pm\delta}$ (M= Ag, Ce, Sr; x=0, 0.3; y=0, 0.2) CATALYST

4.1.1.1 X-Ray diffraction pattern

The XRD pattern of $\text{La}_{1-x}\text{Ag}_x\text{Co}_{1-y}\text{Bi}_y\text{O}_{3\pm\delta}$ (x =0, 0.3; y=0, 0.2) catalysts prepared by co-precipitation are represented in Figs. 4.1, 4.2. Fig shows the prominent peaks of perovskite phase at $2\theta = 23.5, 33, 40.5, 47.5, 59, 70, 78.5$. La_2O_3 peaks were observed at $2\theta = 27.5, 68$. Ag_2O peaks could be identified at $2\theta = 54.5$. While peaks corresponds to Co_3O_4 and Bi_2O_5 could be observed at $2\theta = 44.5, 59.5, 79$ and 53 . For catalysts prepared by dry mixing method also prominent sharp peaks of perovskite could be observed at $2\theta = 23.5$. From these XRDs, the formation of substituted perovskites were confirmed by the method of elimination by showing the absence of individual oxide peaks and peaks with greater intensity and places other than those. This method was adopted in view of the absence of d values for the substituted perovskites considered in the present work, in the JCPDS files (1971).

4.1.1.2 Scanning Electron Micrographs

Fig 4.3 and 4.4 presents the scanning electron micrographs of $\text{La}_x\text{Ag}_{1-x}\text{Co}_y\text{Bi}_{1-y}\text{O}_{3\pm\delta}$ catalysts prepared by co-precipitation. The micrographs shows variations in size and morphology of the samples.

4.1.1.3 Thermal studies

Thermal gravimetric analysis (TGA), differential thermal analysis (DTA) and derivative thermo gravimetric analysis (DTGA) of A-site and B-site substituted perovskite catalysts were presented in Fig 4.3 and 4.4. TGA curve 3(a) for $\text{La}_{0.7}\text{Ag}_{0.3}\text{Co}_{0.8}\text{Bi}_{0.2}\text{O}_{3\pm\delta}$ precursor precipitate sample heated at 10°C per minute in air

environment from ambient temperature to 1000°C shows weight loss at around initial stages of heating which continued gradually up to 350°C and there after weight is increased up to 880°C and then there is a sudden increase in weight loss up to 930°C.

DTA curve 3(b) shows there is no particular endotherm. But an accelerated endotherm was observed with in the heating range.

DTGA curve 3(c) reletates correspondences with TGA and DTA curves for the precipitate of $\text{La}_{0.7}\text{Ag}_{0.3}\text{Co}_{0.8}\text{Bi}_{0.2}\text{O}_{3\pm\delta}$. The DTGA curve shows an increase in weight during 900°C-930°C and then there is a sudden increase in weight loss during 930°C - 960°C. From the TG curve we can observe that there is no much loss in weight.

4.1.2 CATALYTIC ACTIVITY STUDIES

4.1.2.1 Catalytic activity of $\text{La}_{1-x}\text{Ag}_x\text{Co}_{1-y}\text{Bi}_y\text{O}_{3\pm\delta}$ (x =0, 0.3; y=0, 0.2) catalyst prepared by co-precipitation for CO oxidation.

The substituted perovskite catalysts at both A- and B-site with Ag and Bi (B-site) were tested for CO conversion. Fig 4.7 shows the % CO conversion of $\text{La}_{1-x}\text{Ag}_x\text{Co}_{1-y}\text{Bi}_y\text{O}_{3\pm\delta}$ (x =0, 0.3; y=0, 0.2) catalysts. These catalysts were prepared by co-precipitation method and calcined at 800°C for 6h. Three characteristic temperatures namely T_{10} , T_{50} and T_{100} were taken as bench marks for catalyst performance evaluation. Table 4.1 represents the characteristic temperatures of $\text{La}_{1-x}\text{Ag}_x\text{Co}_{1-y}\text{Bi}_y\text{O}_{3\pm\delta}$ (x =0,0.3; y=0,0.2) catalysts. Among these catalysts $\text{La}_{0.7}\text{Ag}_{0.3}\text{Co}_{0.8}\text{Bi}_{0.2}\text{O}_{3\pm\delta}$ showing best performance towards the oxidation of CO on which 100% conversion of CO was obtained at around 165°C. The catalytic activity of these catalysts for the oxidation of CO is in the following order: $\text{La}_{0.7}\text{Ag}_{0.3}\text{Co}_{0.8}\text{Bi}_{0.2}\text{O}_{3\pm\delta} > \text{La}_{0.7}\text{Ag}_{0.3}\text{CoO}_{3\pm\delta} > \text{LaCo}_{0.8}\text{Bi}_{0.2}\text{O}_{3\pm\delta} > \text{LaCoO}_3$.

Table 4.1: Characteristic conversion temperatures for CO oxidation on $\text{La}_{1-x}\text{Ag}_x\text{Co}_{1-y}\text{Bi}_y\text{O}_{3\pm\delta}$ (x =0, 0.3; y=0, 0.2) catalyst prepared by co-precipitation

S.No	catalyst	Characteristic conversion temperature		
		T_{10}	T_{50}	T_{100}
1	LaCoO_3	148	228	---
2	$\text{La}_{0.7}\text{Ag}_{0.3}\text{CoO}_3$	76	134	225.5
3	$\text{La}_{0.7}\text{Ag}_{0.3}\text{Co}_{0.8}\text{Bi}_{0.2}\text{O}_{3\pm\delta}$	77	104	165
4	$\text{LaCo}_{0.8}\text{Bi}_{0.2}\text{O}_{3\pm\delta}$	105	166	272

4.1.2.2 Catalytic activity of $\text{La}_{1-x}\text{Ag}_x\text{Co}_{1-y}\text{Bi}_y\text{O}_{3\pm\delta}$ ($x = 0, 0.3; y=0, 0.2$) catalyst prepared by dry-mixing method for CO oxidation.

The Catalytic activity of $\text{La}_{1-x}\text{Ag}_x\text{Co}_{1-y}\text{Bi}_y\text{O}_{3\pm\delta}$ ($x = 0, 0.3; y=0, 0.2$) were tested for CO oxidation. The catalysts were prepared by dry-mix method and calcined at different terminal temperatures like 250°C, 500°C and 800°C. Fig 4.8 represents the catalytic activity of $\text{La}_{1-x}\text{Ag}_x\text{Co}_{1-y}\text{Bi}_y\text{O}_{3\pm\delta}$ ($x = 0, 0.3; y=0, 0.2$) catalysts at different temperature for CO oxidation. By comparing the catalytic activity of these catalysts from Fig 4.8 and Table 4.2, $\text{La}_{0.7}\text{Ag}_{0.3}\text{Co}_{0.8}\text{Bi}_{0.2}\text{O}_{3\pm\delta}$ showing best performance towards the oxidation of CO on which the complete conversion of CO is obtained at around 198°C. The catalytic activity of these catalysts on the oxidation of CO is in the following order: $\text{La}_{0.7}\text{Ag}_{0.3}\text{Co}_{0.8}\text{Bi}_{0.2}\text{O}_{3\pm\delta} > \text{La}_{0.7}\text{Ag}_{0.3}\text{CoO}_{3\pm\delta} > \text{LaCo}_{0.8}\text{Bi}_{0.2}\text{O}_{3\pm\delta} > \text{LaCoO}_3$.

Table 4.2: Characteristic conversion temperatures for CO oxidation on $\text{La}_{1-x}\text{Ag}_x\text{Co}_{1-y}\text{Bi}_y\text{O}_{3\pm\delta}$ ($x = 0, 0.3; y=0, 0.2$) catalyst prepared by dry-mixing method

S.No	catalyst	Characteristic conversion temperature		
		T ₁₀	T ₅₀	T ₁₀₀
1	LaCoO_3	96	212	-
2	$\text{La}_{0.7}\text{Ag}_{0.3}\text{CoO}_3$	75	118	226
3	$\text{La}_{0.7}\text{Ag}_{0.3}\text{Co}_{0.8}\text{Bi}_{0.2}\text{O}_{3\pm\delta}$	-	110	198
4	$\text{LaCo}_{0.8}\text{Bi}_{0.2}\text{O}_{3\pm\delta}$	79.5	179.5	276.5

4.1.2.3 Catalytic activity of $\text{La}_{1-x}\text{Ce}_x\text{Co}_{1-y}\text{Bi}_y\text{O}_{3\pm\delta}$ ($x = 0, 0.3; y=0, 0.2$) catalysts for CO oxidation.

The Ce- and Bi- substituted lanthanum cobaltate perovskites were tested for CO conversion. The Ce- and Bi-substituted perovskites has the formula $\text{La}_{1-x}\text{Ce}_x\text{Co}_{1-y}\text{Bi}_y\text{O}_{3\pm\delta}$ ($x = 0, 0.3; y=0, 0.2$). The catalysts were prepared by co-precipitation method and calcined at different terminal temperatures like 250°C, 500°C and 800°C. The catalytic activity tests were performed in the temperature range of 50°-300°C at a space velocity of

19850h⁻¹. The performance of these catalysts for the oxidation of CO was represented by Fig 4.9 and Table 4.3. The perovskite catalyst substituted with Ce and Bi at A- and B-sites showing very good activity for the low temperature oxidation of CO. the 100% conversion of CO is observed at around 186°C. The catalytic activity of these catalysts on the oxidation of CO is in the following order: La_{0.7}Ce_{0.3}Co_{0.8}Bi_{0.2}O_{3±δ} > La_{0.7}Ce_{0.3}CoO_{3±δ} > LaCo_{0.8}Bi_{0.2}O_{3±δ} > LaCoO₃.

Table 4.3: Characteristic conversion temperatures for CO oxidation on La_{1-x}Ce_xCo_{1-y}Bi_yO_{3±δ} (x =0, 0.3; y=0, 0.2)

S.No	catalyst	Characteristic conversion temperature		
		T ₁₀	T ₅₀	T ₁₀₀
1	LaCoO ₃	148	228	-
2	La _{0.7} Ce _{0.3} CoO ₃	-	114.5	198
3	La _{0.7} Ce _{0.3} Co _{0.8} Bi _{0.2} O _{3±δ}	-	105.5	186
4	LaCo _{0.8} Bi _{0.2} O _{3±δ}	105	166	272

4.1.2.4 Catalytic activity of La_{1-x}Sr_xCo_{1-y}Bi_yO_{3±δ} (x =0, 0.3; y=0, 0.2) catalysts for CO and C₃H₆ oxidation.

The catalytic results of La_{1-x}Sr_xCo_{1-y}Bi_yO_{3±δ} (x =0, 0.3; y=0, 0.2) perovskite catalysts for oxidation of CO and C₃H₆ were summarized in Table 4.4 by means of the 10%, 50% and 100% conversion temperatures. The conversion curves of oxidation of CO and C₃H₆ over these catalysts are shown in Fig 4.10 and 4.11 respectively. The catalysts were prepared by co-precipitation method and calcined at different terminal temperatures like 250°C, 500°C and 800°C. The catalytic activity tests were performed in the temperature range of 50°C-300°C at a space velocity of 19850h⁻¹. Among these catalysts La_{0.7}Sr_{0.3}Co_{0.8}Bi_{0.2}O_{3±δ} showing best performance towards the oxidation of CO and C₃H₆ on which the 100% conversion of CO and C₃H₆ is observed at 200°C and 298°C.

Table 4.4: Characteristic conversion temperatures for CO and C₃H₆ oxidation on La_{1-x}Sr_xCo_{1-y}Bi_yO_{3±δ} (x =0, 0.3; y=0, 0.2)

S.No	catalyst	Characteristic conversion temperature					
		CO			C ₃ H ₆		
		T ₁₀	T ₅₀	T ₁₀₀	T ₁₀	T ₅₀	T ₁₀₀
1	LaCoO ₃	148	228	-	134.2	241	-
2	La _{0.7} Sr _{0.3} CoO ₃	-	121	225	101	176	-
3	La _{0.7} Sr _{0.3} Co _{0.8} Bi _{0.2} O _{3±δ}	-	110	200	92	151.4	298
4	LaCo _{0.8} Bi _{0.2} O _{3±δ}	105	166	272	119.8	187.4	-

4.1.2.5 Performance of La_{1-x}Ag_xCo_{0.8}Bi_{0.2}O_{3±δ} (x=0, 0.3) catalyst prepared by co-precipitation method for CO and C₃H₆ oxidation.

The performance of La_{1-x}Ag_xCo_{0.8}Bi_{0.2}O_{3±δ}(x=0, 0.3) for the oxidation of CO and C₃H₆ is represented by Fig 4.12, 4.13 and Table 4.5. The activity tests were performed at a space velocity of 19850h⁻¹. The activity of the prepared catalyst calcined at 800°C increases with increasing of x value in La_xAg_{1-x}Co_{0.8}Bi_{0.2}O_{3±δ} (x=0, 0.3). The catalytic activity appeared to be depend directly on the content of Ag. The 100% conversion of CO and C₃H₆ on La_{0.6}Ag_{0.4}Co_{0.8}Bi_{0.2}O_{3±δ} is observed at around 168°C and 280°C.

Table 4.5: Characteristic conversion temperatures for CO oxidation on La_xAg_{1-x}Co_{0.8}Bi_{0.2}O_{3±δ} (x =0.1- 0.4)

S.No	catalyst	Characteristic conversion temperature					
		CO			C ₃ H ₆		
		T ₁₀	T ₅₀	T ₁₀₀	T ₁₀	T ₅₀	T ₁₀₀
1	La _{0.9} Ag _{0.1} Co _{0.8} Bi _{0.2} O _{3±δ}	76	108.5	199	119.3	214.3	-
2	La _{0.8} Ag _{0.2} Co _{0.8} Bi _{0.2} O _{3±δ}	-	106.5	175	111.7	194.4	-
3	La _{0.7} Ag _{0.3} Co _{0.8} Bi _{0.2} O _{3±δ}	77	104	165	95	168.5	-
4	La _{0.6} Ag _{0.4} Co _{0.8} Bi _{0.2} O _{3±δ}	-	93	168	81	139	280

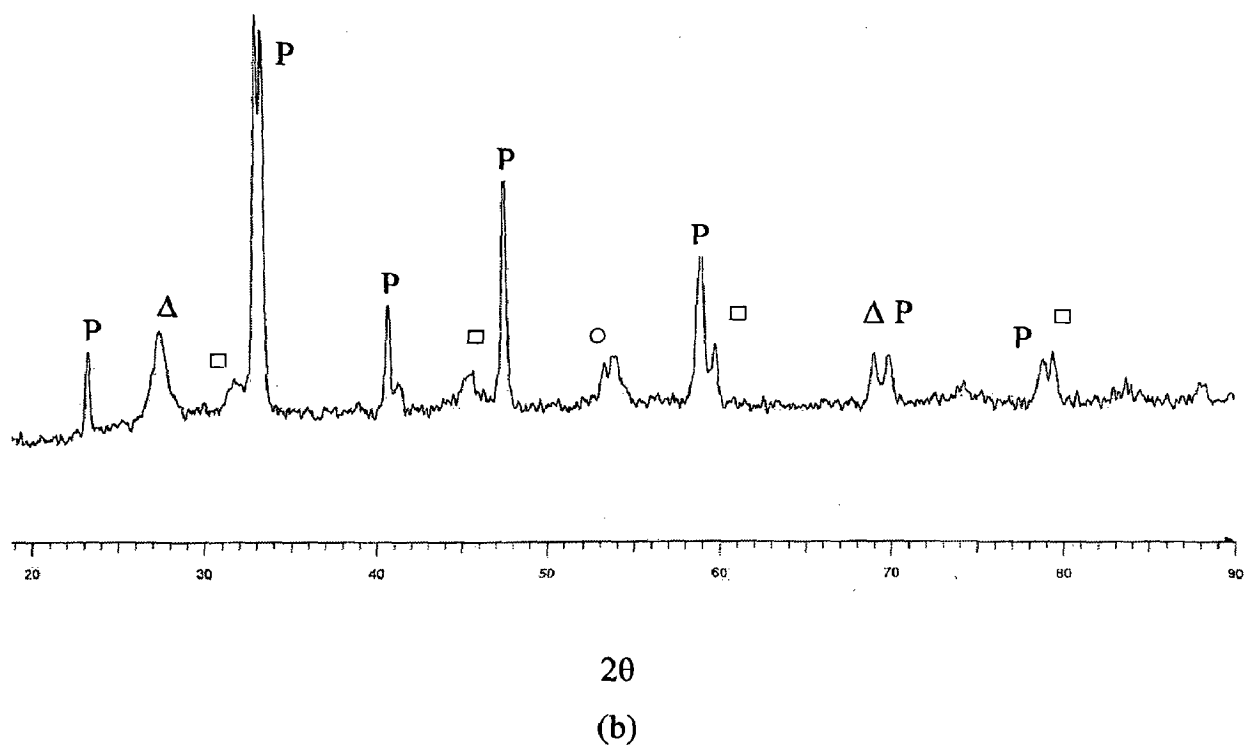
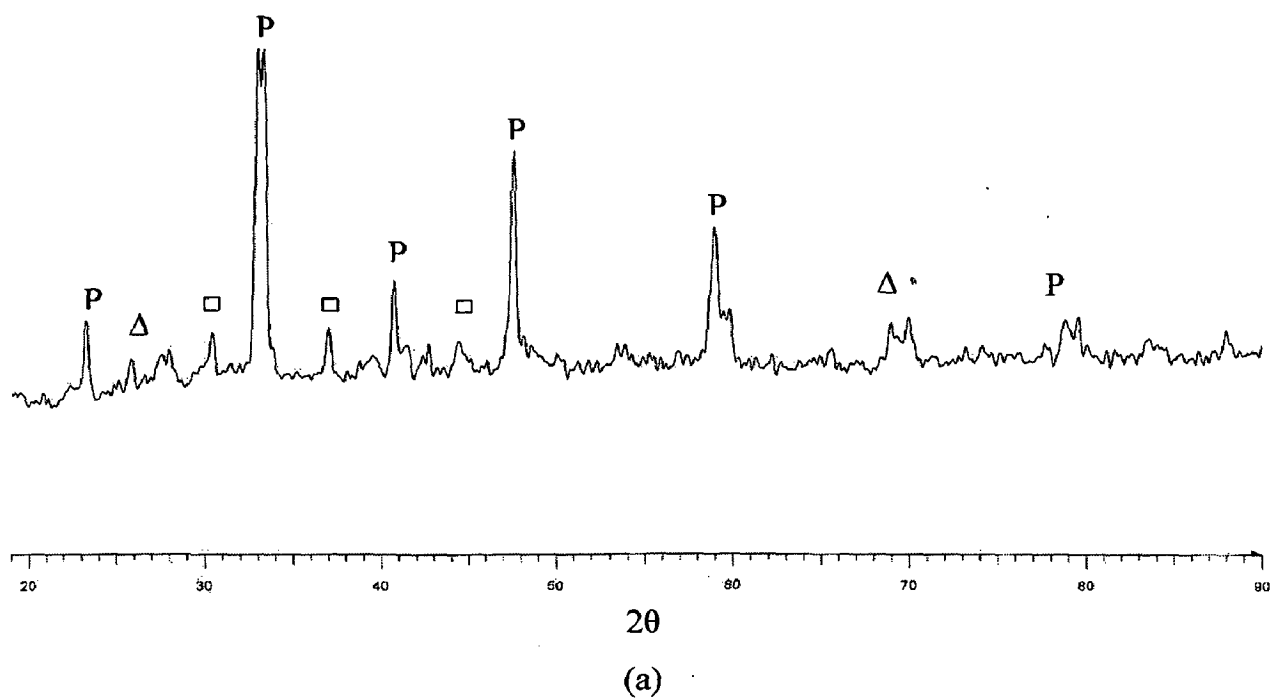
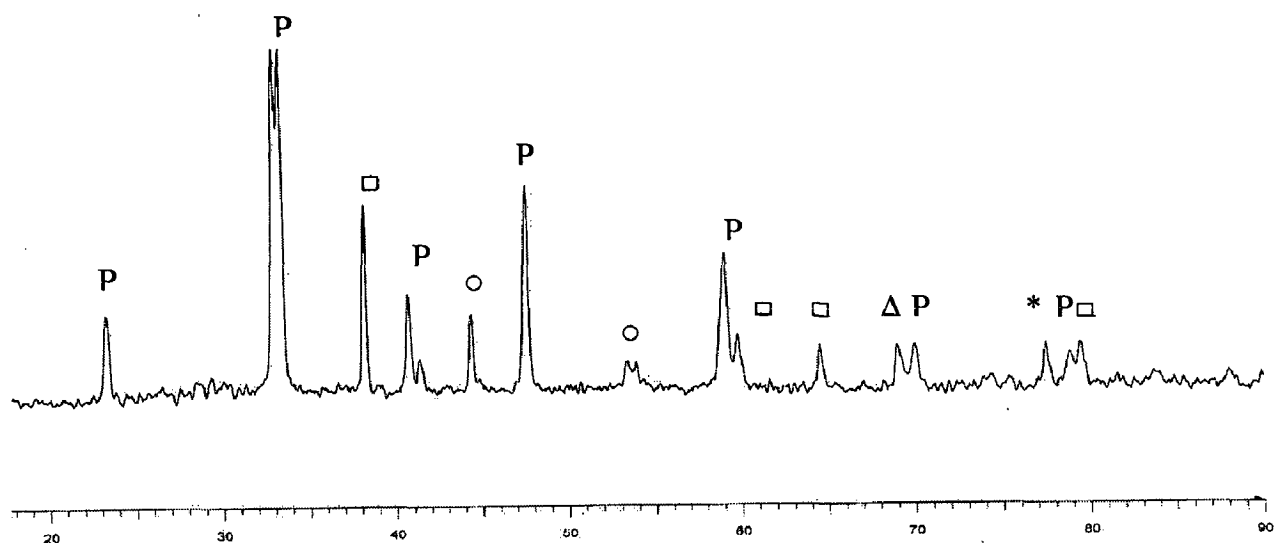
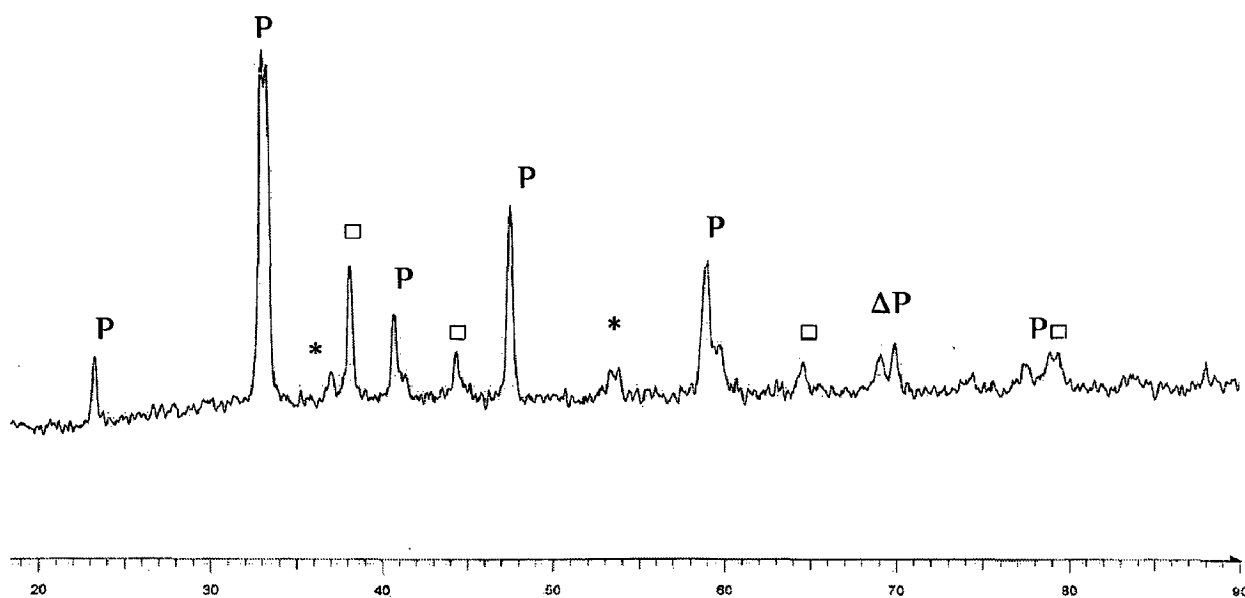


Fig 4.1: X-ray diffraction pattern of (a) LaCoO_3 (b) $\text{La}_{0.7}\text{Ag}_{0.3}\text{CoO}_{3\pm\delta}$ calcined at 800°C , P: perovskite; \square : Co_3O_4 ; Δ : La_2O_3 ; \circ Ag_2O_3 , * Bi_3O_4



2θ

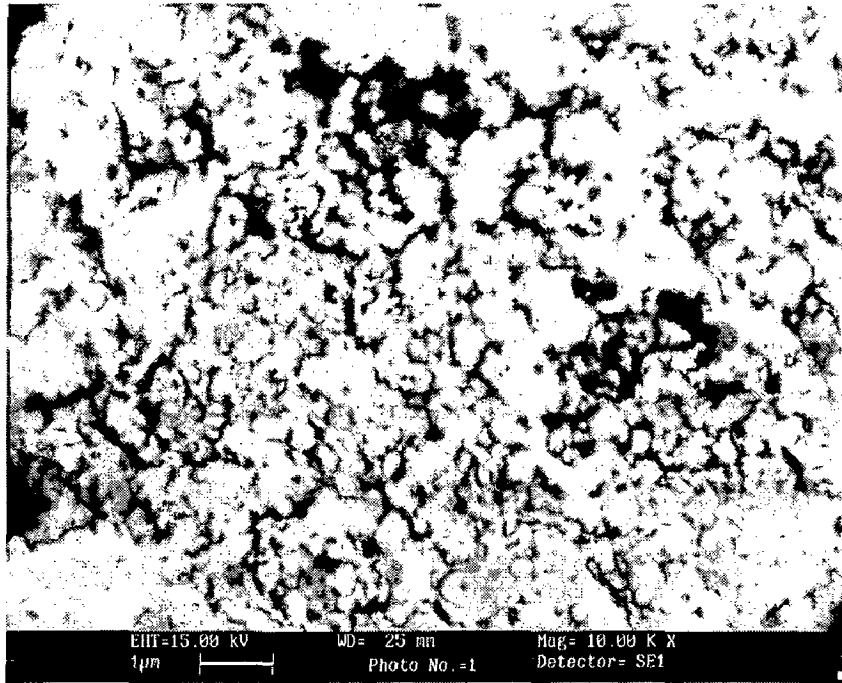
(c)



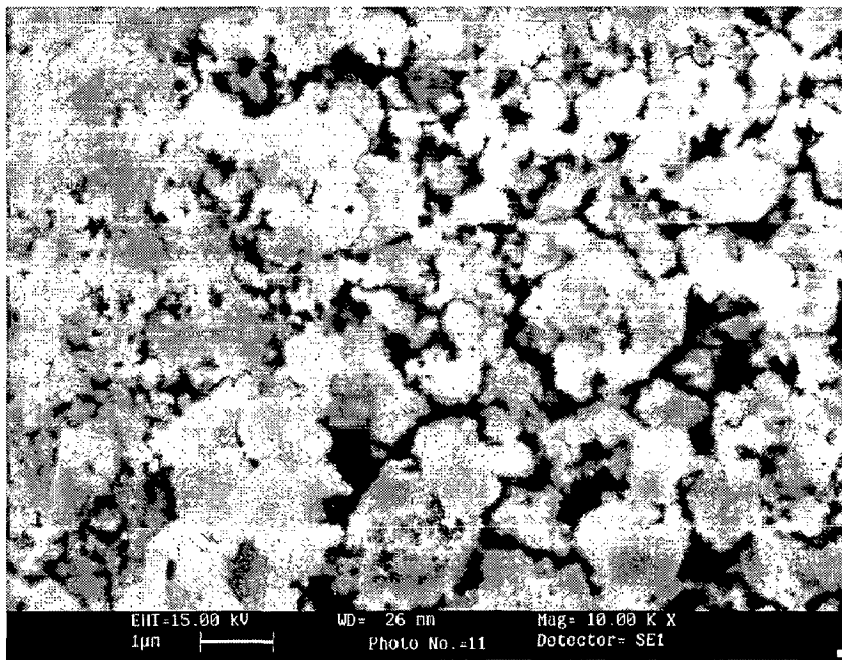
2θ

(d)

Fig 4.2: X-ray diffraction pattern of (c) $\text{La}_{0.7}\text{Ag}_{0.3}\text{Co}_{0.8}\text{Bi}_{0.2}\text{O}_{3\pm\delta}$ (d) $\text{LaCo}_{0.8}\text{Bi}_{0.2}\text{O}_{3\pm\delta}$ calcined at 800°C , P: perovskite; □: Co_3O_4 ; Δ: La_2O_3 ; ○ Ag_2O_3 , * Bi_3O_4

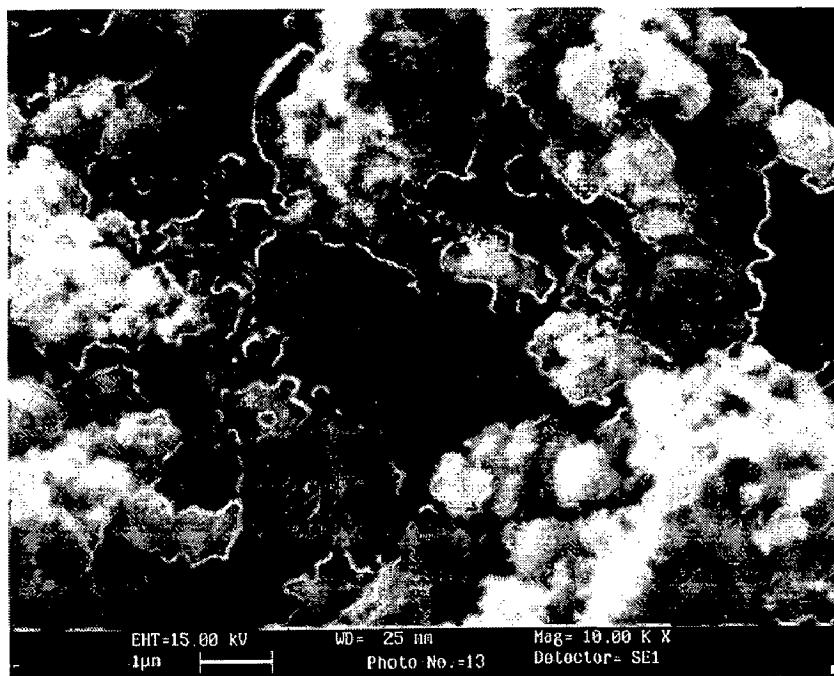


(a)

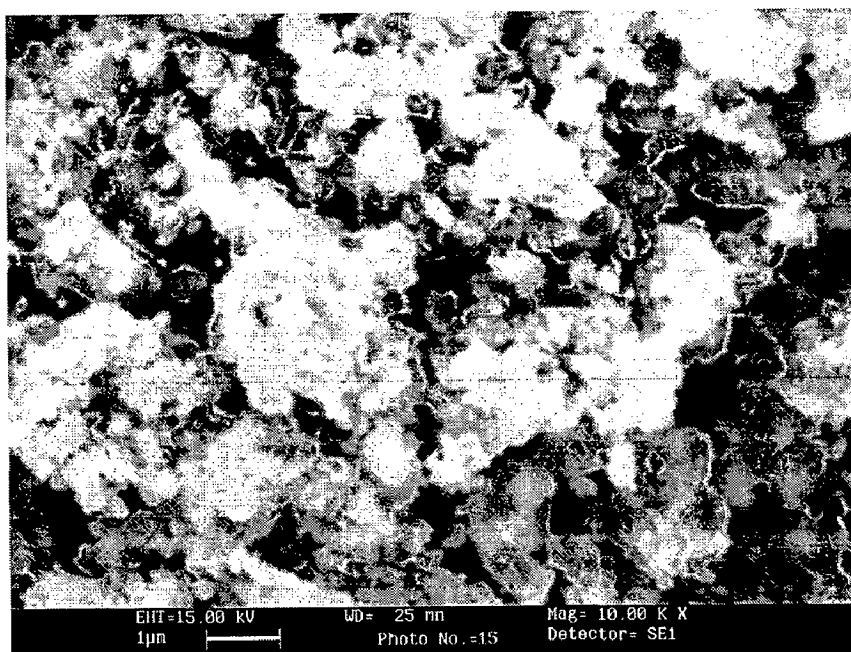


(b)

Fig 4.3: SEM images of (a) LaCoO_3 (b) $\text{La}_{0.7}\text{Ag}_{0.3}\text{CoO}_3$ catalysts prepared by co-precipitation method and calcined at 800°C at 10KX

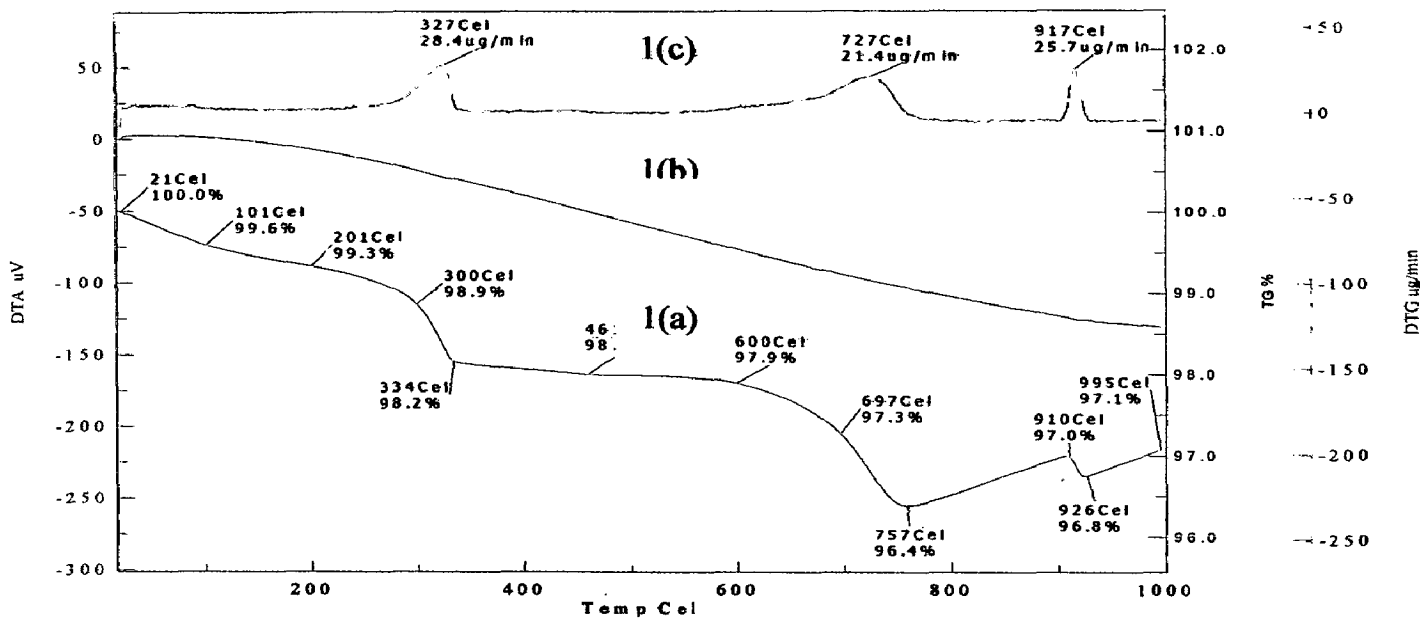


(c)

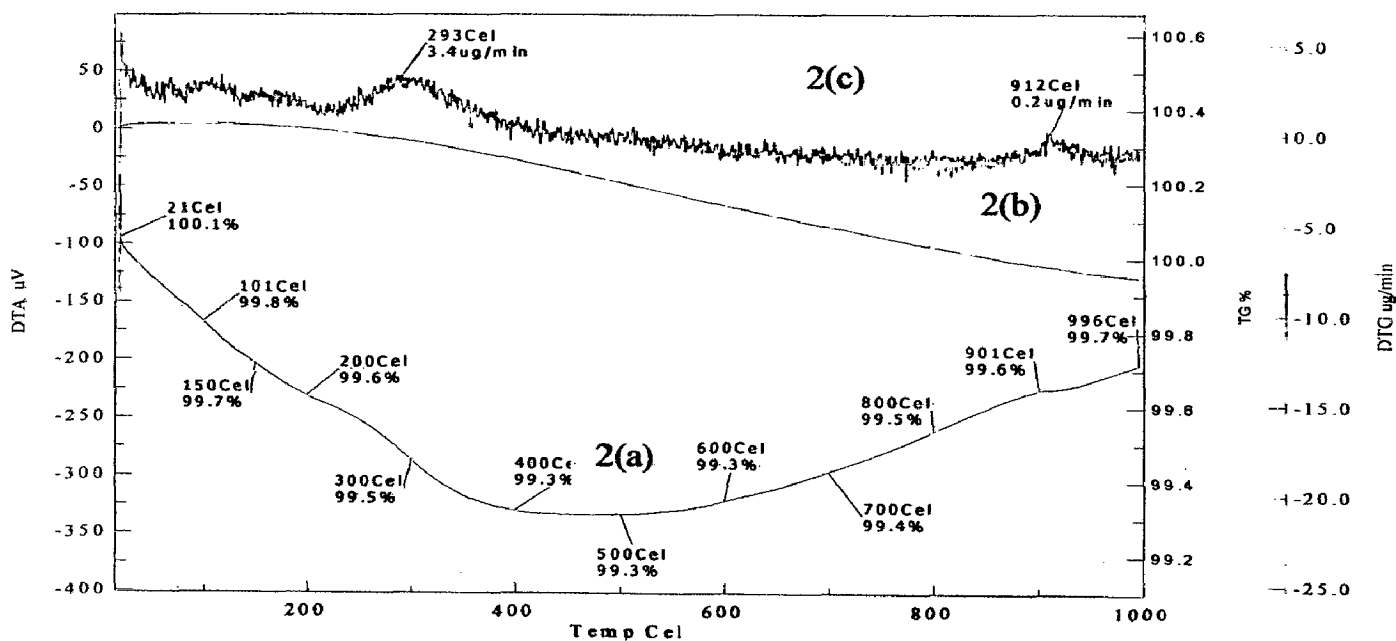


(d)

Fig 4.4: SEM images of (c) $\text{La}_{0.7}\text{Ag}_{0.3}\text{Co}_{0.8}\text{Bi}_{0.2}\text{O}_3$ (b) $\text{LaCo}_{0.8}\text{Bi}_{0.2}\text{O}_3$ catalysts prepared by co-precipitation method and calcined at 800°C at 10KX

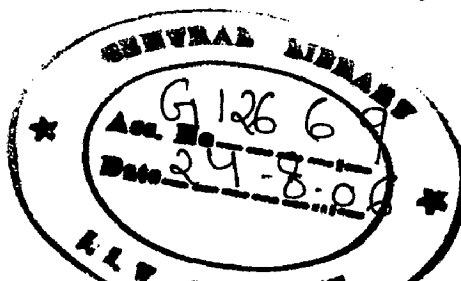


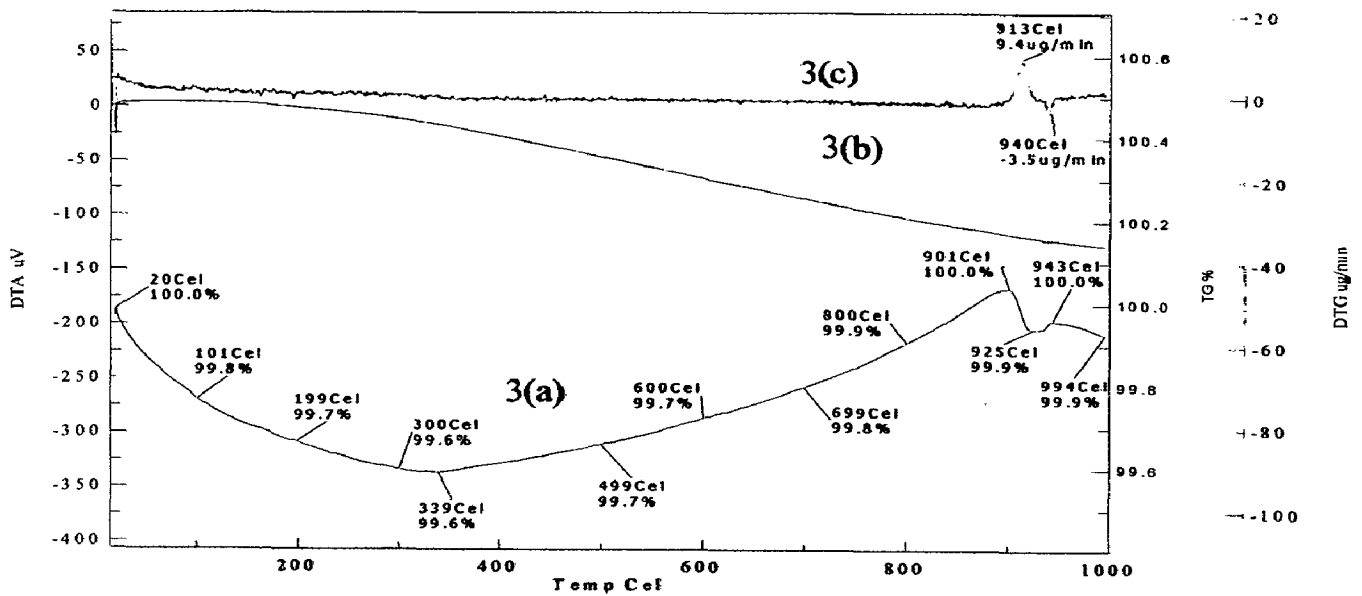
(1)



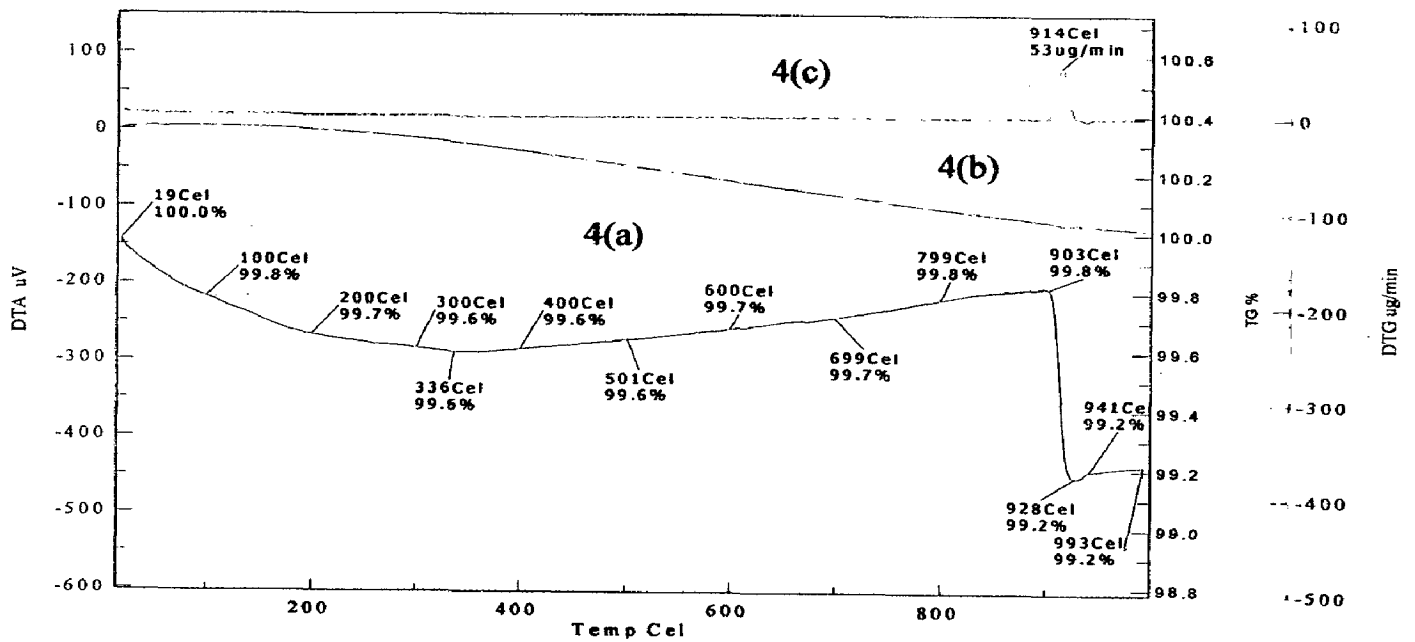
(2)

Fig 4.5: Thermo gravimetric (a), Differential thermal (b), Derivative thermo gravimetric (c) analysis of (1) LaCoO₃, (2) La_{0.7}Ag_{0.3}CoO₃ catalysts





(3)



(4)

Fig 4.6: Thermo gravimetric (a), Differential thermal (b), Derivative thermo gravimetric (c) analysis of (3) $\text{La}_{0.7}\text{Ag}_{0.3}\text{Co}_{0.8}\text{Bi}_{0.2}\text{O}_3$, (4) $\text{LaCo}_{0.8}\text{Bi}_{0.2}\text{O}_3$ catalysts

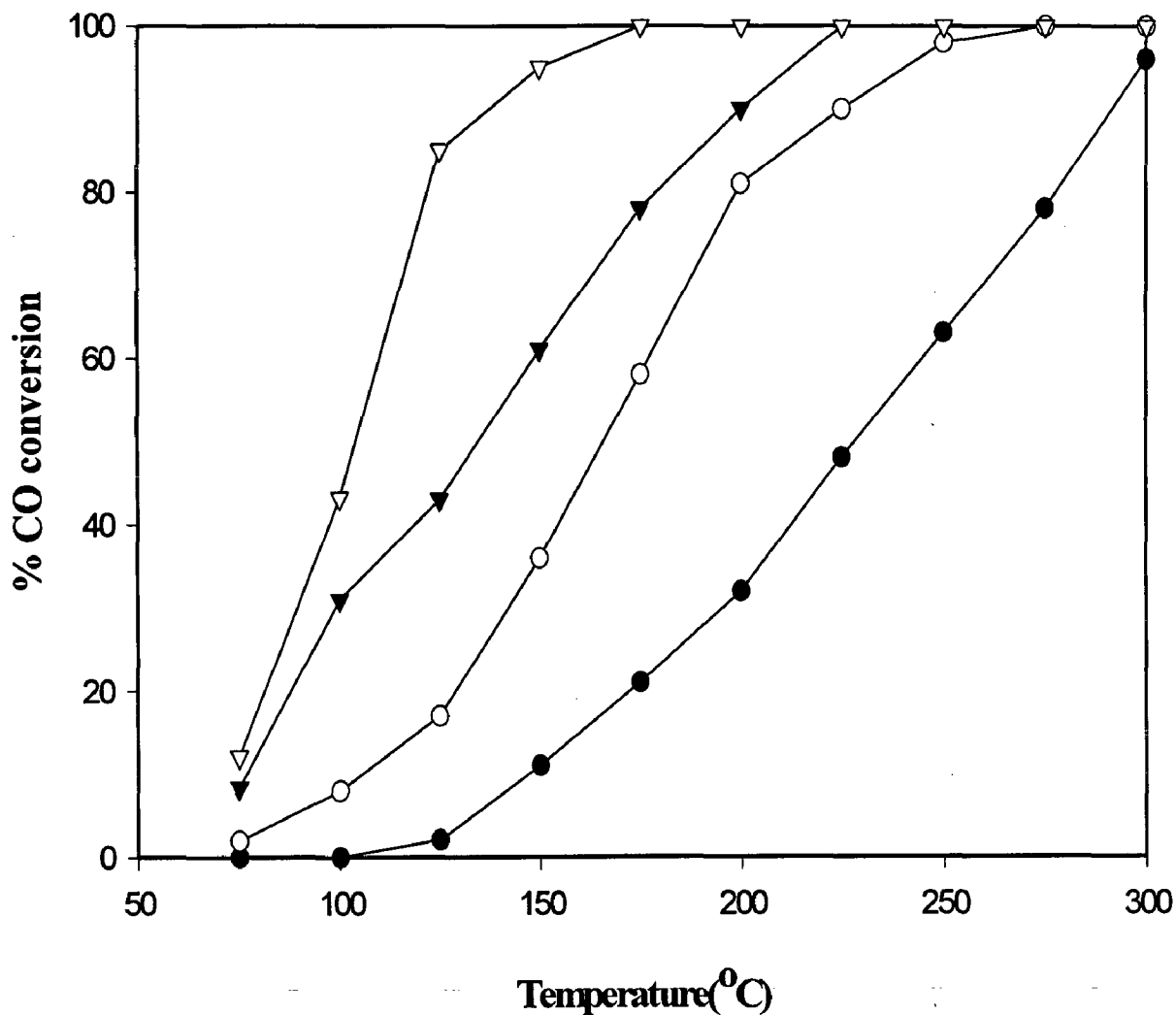


Fig 4.7: Comparison of catalytic activity of $\text{La}_{1-x}\text{Ag}_x\text{Co}_{1-y}\text{Bi}_y\text{O}_{3\pm\delta}$ ($x=0, 0.3$; $y=0, 0.2$) catalysts prepared by co-precipitation method and calcined at 800°C for the oxidation of CO

Space velocity: 19850 h^{-1}

▼: $\text{La}_{0.7}\text{Ag}_{0.3}\text{CoO}_3$;

●: LaCoO_3 ;

○: $\text{LaCo}_{0.8}\text{Bi}_{0.2}\text{O}_3$;

▽: $\text{La}_{0.7}\text{Ag}_{0.3}\text{Co}_{0.8}\text{Bi}_{0.2}\text{O}_3$

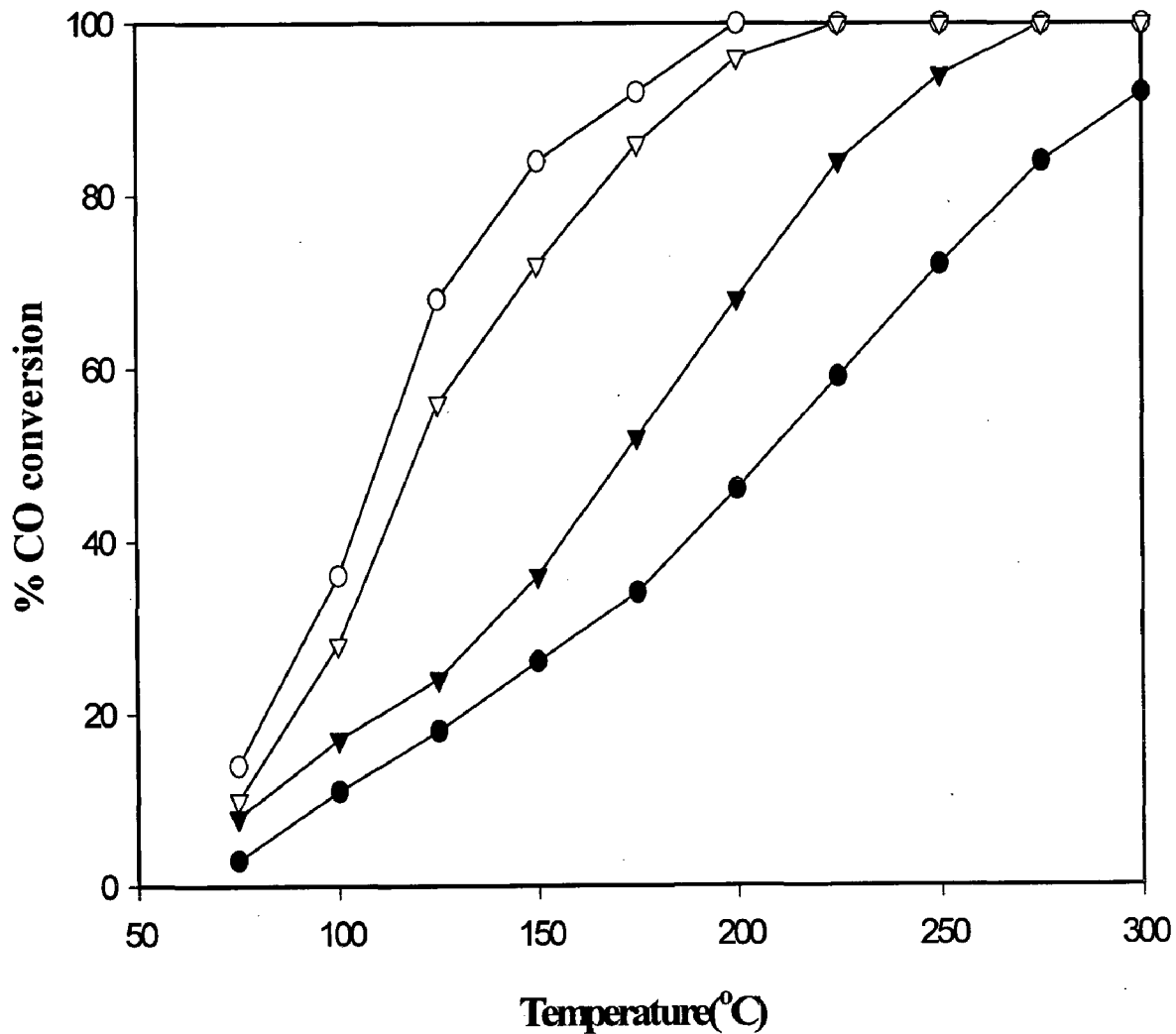


Fig 4.8: Comparison of catalytic activity of $\text{La}_{1-x}\text{Ag}_x\text{Co}_{1-y}\text{Bi}_y\text{O}_{3\pm\delta}$ ($x=0, 0.3$; $y=0, 0.2$) catalyst prepared by dry mixing method for the oxidation of CO

Space velocity: 19850 h^{-1}

▼: $\text{LaCo}_{0.8}\text{Bi}_{0.2}\text{O}_3$;

●: LaCoO_3 ;

○: $\text{La}_{0.7}\text{Ag}_{0.3}\text{Co}_{0.8}\text{Bi}_{0.2}\text{O}_3$;

▽: $\text{La}_{0.7}\text{Ag}_{0.3}\text{CoO}_3$

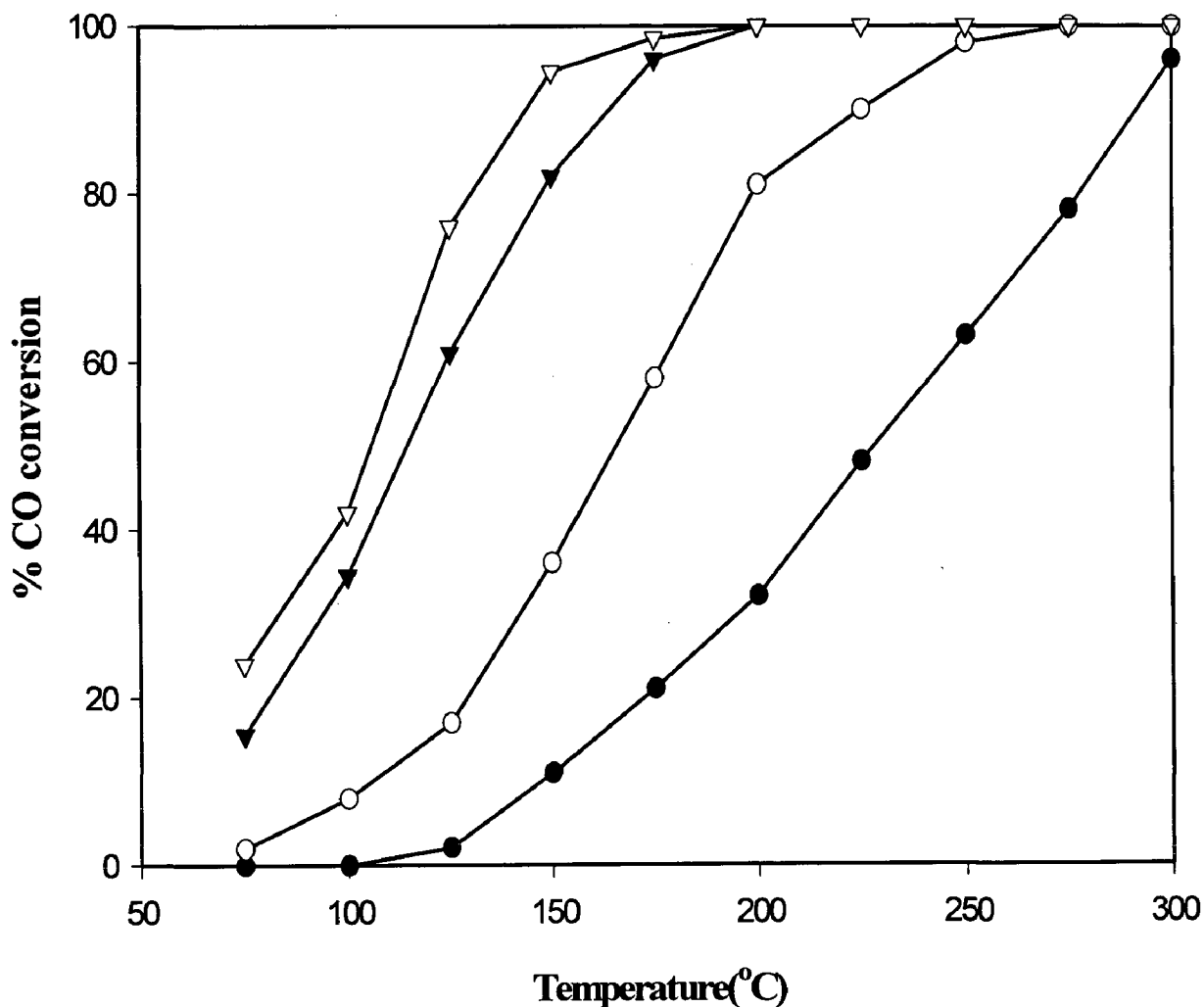


Fig 4.9: Comparison of catalytic activity of $\text{La}_{1-x}\text{Ce}_x\text{Co}_{1-y}\text{Bi}_y\text{O}_{3\pm\delta}$ ($x=0, 0.3; y=0, 0.2$) catalyst prepared by co-precipitation method for the oxidation of CO

Space velocity: 19850h^{-1}

▼: $\text{La}_{0.7}\text{Ce}_{0.3}\text{CoO}_3$;

●: LaCoO_3 ;

○: $\text{LaCo}_{0.8}\text{Bi}_{0.2}\text{O}_3$;

▽: $\text{La}_{0.7}\text{Ce}_{0.3}\text{Co}_{0.8}\text{Bi}_{0.2}\text{O}_3$.

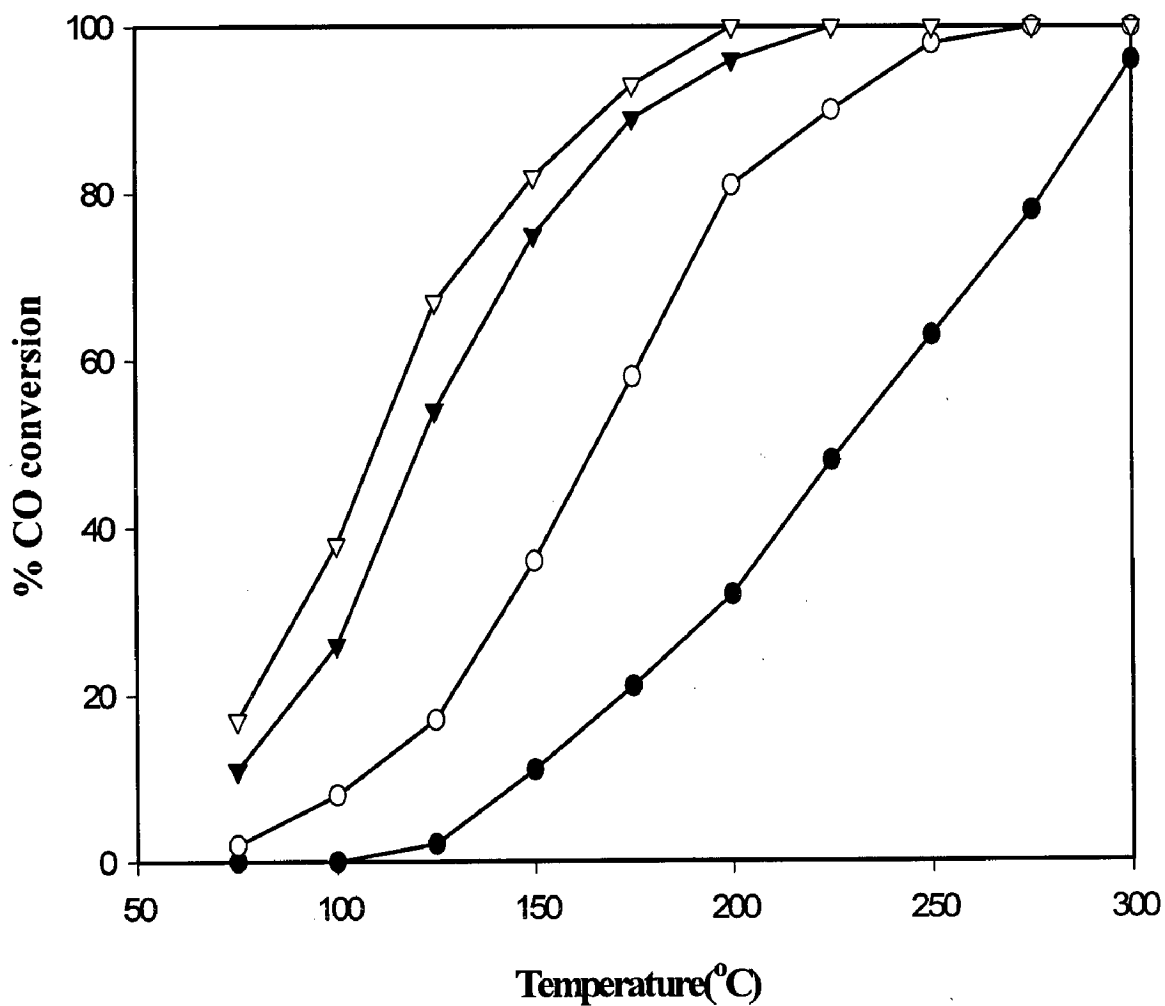


Fig 4.10: Comparison of catalytic activity of $\text{La}_x\text{Sr}_{1-x}\text{Co}_y\text{Bi}_{1-y}\text{O}_{3\pm\delta}$ ($x=0, 0.3$; $y=0, 0.2$) catalyst prepared by co-precipitation method for the oxidation of CO

Space velocity: 19850h^{-1}

▼: $\text{La}_{0.7}\text{Sr}_{0.3}\text{CoO}_3$;

●: LaCoO_3 ;

○: $\text{LaCo}_{0.8}\text{Bi}_{0.2}\text{O}_3$;

▽: $\text{La}_{0.7}\text{Sr}_{0.3}\text{Co}_{0.8}\text{Bi}_{0.2}\text{O}_3$

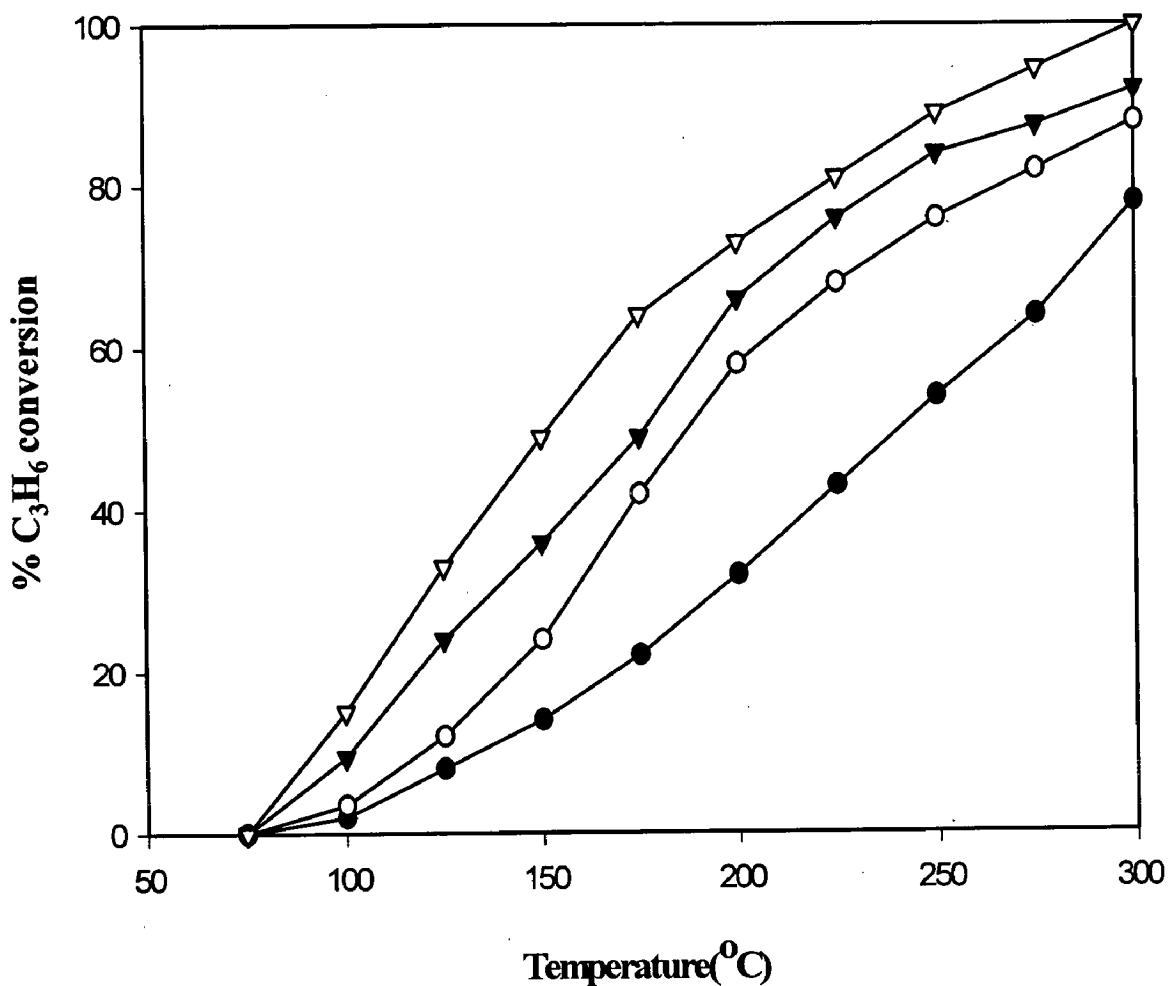


Fig 4.11: Comparison of catalytic activity of $\text{La}_x\text{Sr}_{1-x}\text{Co}_y\text{Bi}_{1-y}\text{O}_{3\pm\delta}$ ($x=0, 0.3$; $y=0, 0.2$) catalyst prepared by co-precipitation method for the oxidation of C_3H_6

Space velocity: 19850h^{-1}

▼: $\text{La}_{0.7}\text{Sr}_{0.3}\text{CoO}_3$;

●: LaCoO_3 ;

○: $\text{LaCo}_{0.8}\text{Bi}_{0.2}\text{O}_3$;

▽: $\text{La}_{0.7}\text{Sr}_{0.3}\text{Co}_{0.8}\text{Bi}_{0.2}\text{O}_3$

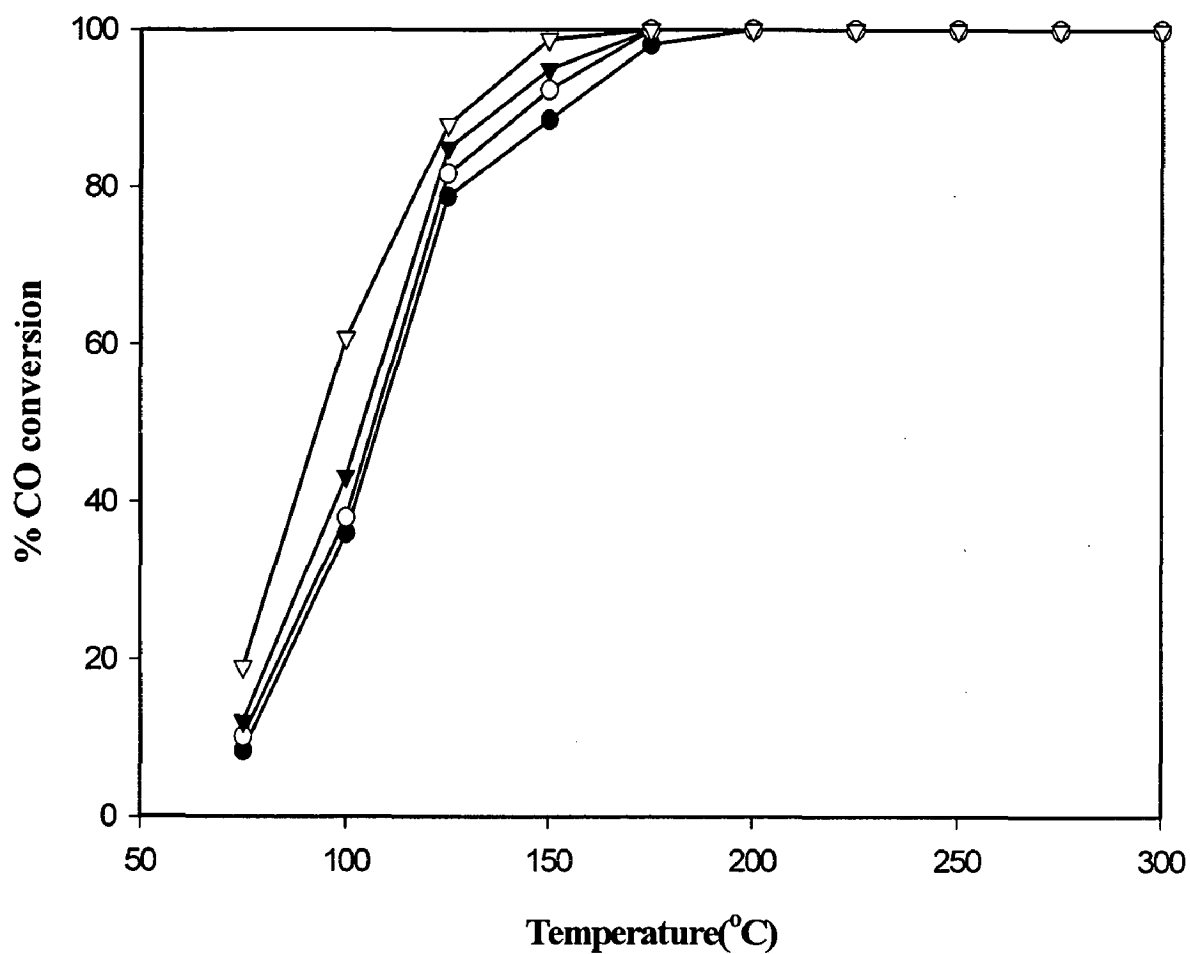


Fig 4.12: Comparison of catalytic activity of $\text{La}_x\text{Ag}_{1-x}\text{Co}_{0.8}\text{Bi}_{0.2}\text{O}_{3\pm\delta}$ ($x = 0.1 - 0.3$) catalyst prepared by co-precipitation method for the oxidation of CO
Space velocity: 19850h^{-1}
▼ : $\text{La}_{0.7}\text{Ag}_{0.3}\text{Co}_{0.8}\text{Bi}_{0.2}\text{O}_3$;
● : $\text{La}_{0.9}\text{Ag}_{0.1}\text{Co}_{0.8}\text{Bi}_{0.2}\text{O}_3$;
○ : $\text{La}_{0.8}\text{Ag}_{0.2}\text{Co}_{0.8}\text{Bi}_{0.2}\text{O}_3$;
▽ : $\text{La}_{0.6}\text{Ag}_{0.4}\text{Co}_{0.8}\text{Bi}_{0.2}\text{O}_3$.

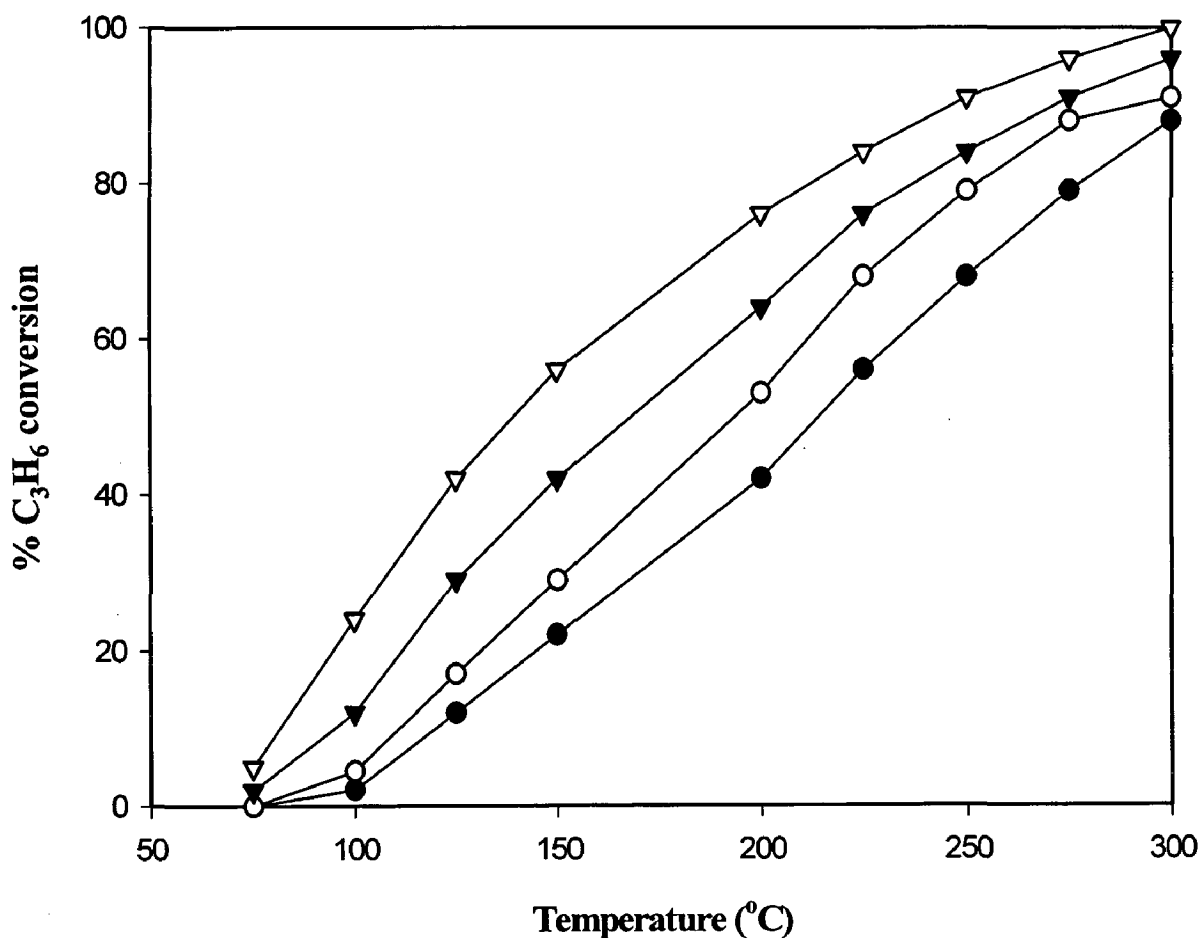


Fig 4.13: Comparison of catalytic activity of $\text{La}_x\text{Ag}_{1-x}\text{Co}_{0.8}\text{Bi}_{0.2}\text{O}_{3\pm\delta}$ ($x = 0.1- 0.3$) catalyst prepared by co-precipitation method for the oxidation of C_3H_6

Space velocity: 19850h^{-1}

▼: $\text{La}_{0.7}\text{Ag}_{0.3}\text{Co}_{0.8}\text{Bi}_{0.2}\text{O}_3$;

●: $\text{La}_{0.9}\text{Ag}_{0.1}\text{Co}_{0.8}\text{Bi}_{0.2}\text{O}_3$;

○: $\text{La}_{0.8}\text{Ag}_{0.2}\text{Co}_{0.8}\text{Bi}_{0.2}\text{O}_3$;

▽: $\text{La}_{0.6}\text{Ag}_{0.4}\text{Co}_{0.8}\text{Bi}_{0.2}\text{O}_3$.

4.2 DISCUSSION

4.2.1 Effect of A- and B- site substitution on the catalytic activity.

The catalytic activity for oxidation and the related properties were generally changed by substitution of La and Co in LaCoO_3 . In this study, substituted perovskite have been prepared by partial substitution of La^{3+} with Ag^+ , Sr^{2+} , Ce^{4+} and Co^{3+} with Bi^{5+} .

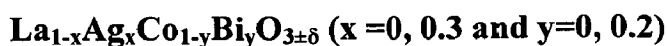
In the perovskite structure ABO_3 , A-cations are believed to be inactive. The partial substitution of A site with lower valency ions can create oxygen vacancies in the perovskite lattice and changes the oxygen state of B site ion. **Dai *et al* (2001)** reported that these substitutions increase the stability of the perovskite structure. The A-site substitutions can be made with Ag^+ , Sr^{2+} , Ce^{4+} . The catalytic activity increased remarkable by the substitution of Ag^+ is observed in the present study, since it creates oxygen deficiency in perovskite structure. The effect of Sr^{2+} , Ce^{4+} substitutions were not profound as compared to that of Ag substitution. When Sr^{2+} is partially substituted for La^{3+} , the charge compensation is effected by the oxidation of Co^{3+} to Co^{4+} and /or formulation of oxygen deficiency is formed by $\text{La}_{1-x}^{3+}\text{Sr}_x^{2+}\text{Co}_{1-x+2\delta}^{3+}\text{Co}_{x-2\delta}^{4+}\text{O}_{3-\delta}$. It has been confirmed by **Nakamura *et al* (1983)**. The oxygen storage property of CeO_2 in the catalyst to diminish the effect of oscillating feed stream between rich and lean exhaust stoichiometries has been recognized by **Gandhi *et al* (1976)**. The oxygen storage capacity (OSC) of CeO_2 is due to its ability to undergo rapid reduction/oxidation cycles of ceria. When cerium is partially substituted for Lanthanum in the LaCoO_3 , part of Co^{3+} is reduced to Co^{2+} .

Dai *et al* (2001) reported that the substitution of Bi for Co enhances the catalytic activity of the perovskite – type oxides significantly. Since Bi^{5+} is bigger than Co^{3+} , the incorporation of Bi^{5+} ions into the B-site would enlarge the perovskite lattice. In the present study, it is observed for the oxidation of CO.

The isostructural partial substitution of A and B-site ions by known ions can modify the nature and concentration of defects in perovskite lattice. A-site substitutions by ions in lower valence induce an increase in oxygen vacancy density (favoring the total oxidation of CO), whereas B-site replacement by Bi^{5+} ion regulate the oxidation state of B-site ion (reinforcing the redox property of the perovskite). Therefore, **He *et al* (2003)**

reported that the simultaneous substitutions of both cationic sites are favorable for the enhancement of CO oxidation. The present study indicates the partial substitution of La^{3+} and Co^{3+} with Ag^+ and Bi^{5+} showing best performance for the oxidation of CO. Fig 4.12 represents the effect of A-site substitution with Ag^+ , Sr^{2+} , Ce^{4+} ion in $\text{LaCo}_{0.8}\text{Bi}_{0.2}\text{O}_{3\pm\delta}$ catalyst for the oxidation of CO.

4.2.2. Effect of method of preparation on the catalytic activity of



The inferior activity of substituted perovskites prepared by dry-mixing method in comparison to the perovskites prepared by co-precipitation method may be attributed to the intermediate grinding, pelletization and calcination at different terminal temperatures used during the preparation. Former catalysts were calcined at 500oC and 800oC without intermediate grinding, where as the later ones were prepared by calcination at various terminal temperatures with intermediate grinding and pelletization, which might had allowed more interaction between the molecules at A and B-sites, resulting in the better perovskite formation and so a superior performance.

4.2.3. Effect of Ag content on the catalytic activity of $\text{La}_{1-x}\text{Ag}_x\text{Co}_{0.8}\text{Bi}_{0.2}\text{O}_{3\pm\delta}$ (x=0.1-0.4)

Substitution of La in $\text{LaCo}_{0.8}\text{Bi}_{0.2}\text{O}_{3\pm\delta}$ by Ag causes an increase of oxidation activity of the catalyst. In the present study, catalytic activities of $\text{La}_{1-x}\text{Ag}_x\text{Co}_{0.8}\text{Bi}_{0.2}\text{O}_{3\pm\delta}$ (0.1, 0.2 0.3 and 0.4) catalysts were measured to asses the effect of the Ag content on the activity of CO oxidation. The content of Ag substitution in $\text{LaCo}_{0.8}\text{Bi}_{0.2}\text{O}_{3\pm\delta}$ has profound effect on the CO oxidation, since the oxygen deficiency increases as the content of Ag increases. In Fig 4.12, the temperatures at which the conversion of CO becomes 50% are shown as a function of Ag content.

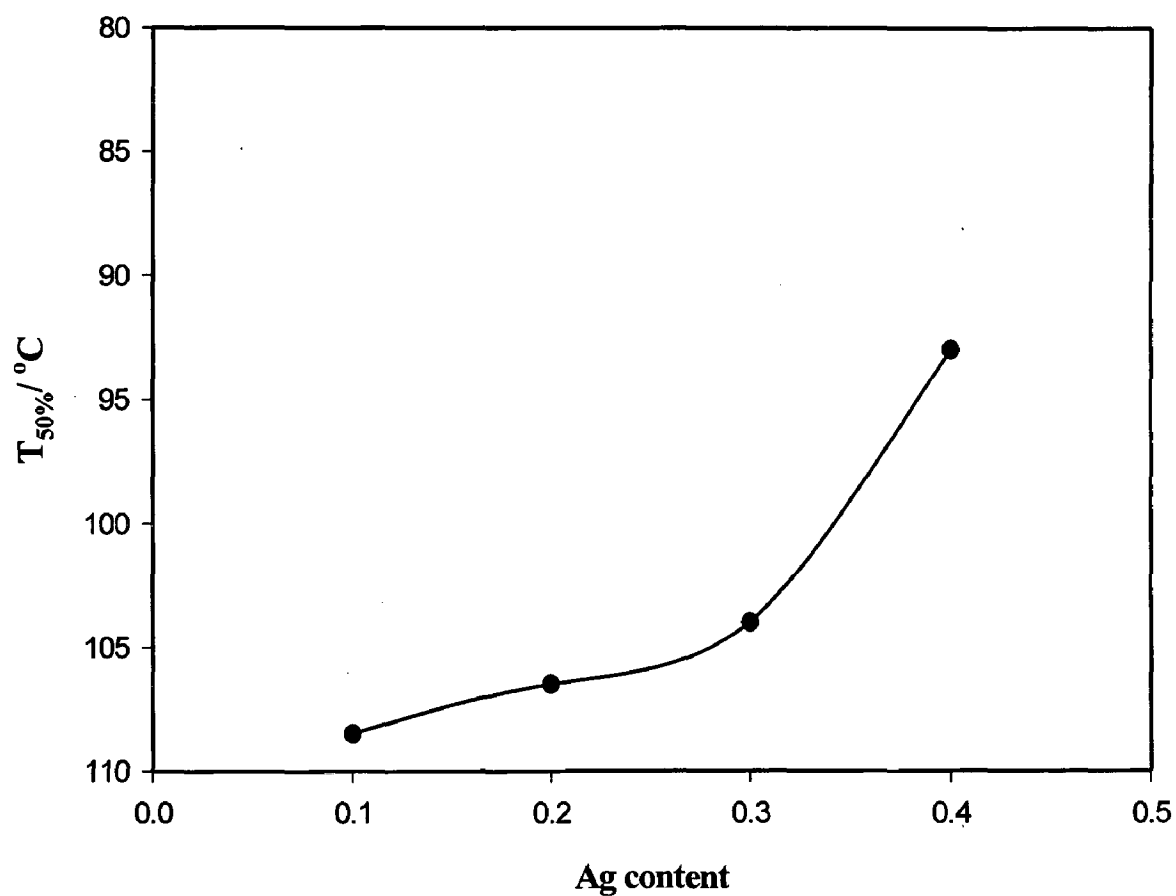


Fig 4.12. The temperature of 50% CO conversion as a function of Ag content in $\text{La}_{1-x}\text{Ag}_x\text{Co}_{0.8}\text{Bi}_{0.2}\text{O}_{3\pm\delta}$

CONCLUSIONS AND RECOMMENDATIONS

5.1 CONCLUSIONS

The following conclusions can be drawn on the basis of the present study on the CO oxidation over substituted perovskite catalysts:

1. Among the $\text{La}_{1-x}\text{Ag}_x\text{Co}_{1-y}\text{Bi}_y\text{O}_{3\pm\delta}$ ($x=0, 0.3; y=0, 0.2$) catalysts prepared by co-precipitation and calcined at 800°C , $\text{La}_{0.7}\text{Ag}_{0.3}\text{Co}_{0.8}\text{Bi}_{0.2}\text{O}_{3\pm\delta}$ is showing best catalytic activity.
2. $\text{La}_{1-x}\text{Ag}_x\text{Co}_{1-y}\text{Bi}_y\text{O}_{3\pm\delta}$ ($x=0, 0.3; y=0, 0.2$) catalysts prepared by co-precipitation method showing best performance in comparison with the dry-mixing method.
3. The Bi incorporated catalysts performed better than Bi-free catalysts.
4. Cerium substituted perovskites showing better performance for the total oxidation of CO. $\text{La}_{0.7}\text{Ce}_{0.3}\text{Co}_{0.8}\text{Bi}_{0.2}\text{O}_{3\pm\delta}$ catalyst showing very good activity among the ceria substituted catalysts
5. Among the Sr^{2+} substituted perovskite catalyst, the order of activity is found as follows: $\text{La}_{0.7}\text{Sr}_{0.3}\text{Co}_{0.8}\text{Bi}_{0.2}\text{O}_{3\pm\delta} > \text{La}_{0.7}\text{Sr}_{0.3}\text{CoO}_{3\pm\delta} > \text{LaCo}_{0.8}\text{Bi}_{0.2}\text{O}_{3\pm\delta} > \text{LaCoO}_3$
6. The content of Ag influence the catalytic activity of $\text{La}_{1-x}\text{Ag}_x\text{Co}_{0.8}\text{Bi}_{0.2}\text{O}_{3\pm\delta}$ ($x=0.1-0.4$) catalysts. At $x=0.4$ the performance of the catalyst is very good for the low temperature oxidation of CO.
7. Ag substituted $\text{LaCo}_{0.8}\text{Bi}_{0.2}\text{O}_3$ catalyst showing better performance in comparison with the Ce and Sr substituted perovskite catalysts, due to its lower oxidation state.

5.2 RECOMMENDATIONS

On the basis of present study the following recommendations can be made for future investigations.

1. The nanoscale catalytic materials can be prepared by using nanoparticle preparation techniques like sol-gel, wet impregnation and combustion synthesis.

- The nanocatalysts have high surface area in comparison with the catalysts prepared by ordinary methods like co-precipitation and dry-mixing methods.
2. The optimization of double substitutions can be done at A-site and B-site in LaCoO_3 perovskite.
 3. The study of the effect of the
 - (i) variation in the feed gas composition.
 - (ii) space velocity particularly in the higher $\text{GHSV} > 40000 \text{h}^{-1}$
 - (iii) and to determine the kinetic mechanism for CO and HC oxidation and NO reduction.
 4. The catalytic activity tests can be performed by replacing the synthetic feed gas mixture with the exhaust from the engine, which is nearer to the actual situation in the field applications.
 5. The study of the stability of the catalysts under more severe environment : longer on -stream-operation at higher temperatures($\sim 500^\circ\text{C}$), subjecting the catalyst to rigorous thermal ageing at higher temperature($> 700^\circ\text{C}$) and longer durations (> 30 hours), under actual exhaust gas environment.
 6. The study of the effect of H_2O vapour and SO_2 on the catalysts performance for the CO and HC oxidation and NO reduction can be done.
 7. Field trials using monoliths and /or packed beds with inert materials to test the performance of the catalysts in actual exhaust conditions for petrol driven two/three wheelers and cars.

REFERENCES

- 1 Chan, K.S., Ma, J., and Chuah, G.K. (1994)**
Catalytic Carbon Monoxide Oxidation over Strontium, Cerium and Copper – Supported Lanthanum Manganates and Cobaltates
Appl. Catal. A: Gen, **197**, pp. 201-227.
- 2 Cimino, S., Lisi, L., Rossi, D.S., Faticanti, M. and Porta. P.(2003)**
Methane combustion and CO oxidation on $\text{LaAl}_{1-x}\text{Mn}_x\text{O}_3$ perovskite-type oxide solid solutions
Appl. Catal. B: Environ, **43**, pp.397-406.
- 3 Du, S.B., Wang, J. and Zhang, H.Y. (1993)**
Structure, Reduction and Catalytic Properties of Perovskite- like $\text{LaMn}_{1-x}\text{Ni}_x\text{O}_3$ oxides.
React. Kinet. Catal. Lett, **81**, No.2, pp. 415-421.
- 4 Dai, H. K., He, H., and Gao. (2001)**
Perovskite-type oxide $\text{ACo}_{0.8}\text{Bi}_{0.2}\text{O}_{2.87}$ (A= $\text{La}_{0.8}\text{Ba}_{0.2}$): A Catalyst for Low Temperature CO oxidation.
Catal. Lett. **73**, pp.149-155.
- 5 Dai, H. K., He, H. and Li, P. H.(2003)**
Highly Active Perovskite-Type oxide $\text{La}_{0.6}\text{Sr}_{0.4}\text{Co}_{0.8}\text{Bi}_{0.2}\text{O}_{2.80}$ Catalyst for CO Low- Temperature Oxidation.
International conference on Catalysis and Environmental pollution control.
- 6 Dahl, L., Jansson, K. and Nygren, M.(1998)**
Preparation, Characterization and Catalytic behavior of Perovskites with nominal Compositions $\text{La}_{1-x}\text{Sr}_x\text{Ga}_{1-2y}\text{Cu}_y\text{Ru}_y\text{O}_{3\pm\delta}$,
Mater. Res. Bull. **33**, pp. 211-222

- 7 **Fujii, H., Mizuno, N. and Miscono, M. (1987)**
Chem. Lett. 1987, pp.2147-2150
- 8 **Florina, C. B., Florin, P., Christophe, J., and Thomas, H.(2002)**
Catalytic properties of $\text{La}_{0.8}\text{A}_{0.2}\text{MnO}_3$ (A= Sr, Ba, K, Cs) and $\text{LaMn}_{0.8}\text{B}_{0.2}\text{O}_3$
(B= Ni, Zn, Cu) perovskites 1. Oxidation of Hydrogen and Propane,
Appl. Catal. B: Environ, **35**, pp.175-183.
- 9 **Gallagher, K. and Johnson, I.W.(1975)**
The activity of $\text{La}_{0.7}\text{Sr}_{0.3}\text{MnO}_3$ without Pt and $\text{La}_{0.7}\text{Pb}_{0.3}\text{MnO}_3$ with varying Pt
contents for the catalytic oxidation of CO.
Mat. Res. Bull. **10**, pp.529-538.
- 10 **Gallagher, K. and Johnson, D.W.(1977)**
J. American Ceramic Society, **60**, pp.28-31.
- 11 **Guilhaume, N., Stefan, D. and Michel. P.(1996)**
Palladium- substituted lanthanum cuprates: application to automotive exhausts
emission purification,
Appl. Catal. B: Environ, **10**, pp.325-344
- 12 **He, H., Dai, H. X. and Au. C. T. (2001)**
An investigation on the utilization of perovskite-type oxides
 $\text{La}_{1-x}\text{Sr}_x\text{MO}_3$ (M= $\text{Co}_{0.77}\text{Bi}_{0.20}\text{Pd}_{0.03}$) as three-way catalysts,
Appl. Catal B: Environ, **33**, pp.65-80
- 13 **Johnson, J. E.W. and Gallagher, P.K.(1973)**
Thermochemica. Acta, **7**, pp.303

- 14 **Johnson, J. E.W., Gallagher, K. and Rhodes, W. W.(1976)**
American ceramic Society Bulletin, **55**, pp.142-147.
- 15 **Johnson, Roy, Kumar, Rakesh and Dharmadhikari. D.M. (1990)**
Catalytic Oxidation of Carbon monoxide and Hydrocarbons on supported Zinc ferrite, journal of IPHE, India, **4**, pp.31-36.
- 16 **Jovanovic, D. and Dondur, V. (1991)**
Three Way Catalytic Activity and Sulfur Tolerance of Single Phase Perovskites in Catalysis and Automotive Pollution Control Studies in Surface Science and Catalysis, (A. crueq and A. Frennet Ed.) Elsevier, Amsterdam, **71**, pp.371-393.
- 17 **Kwang, S. S., Danilo, K. and Jitka. K.(2001)**
Kinetics of propane combustion over $\text{La}_{0.66}\text{Sr}_{0.34}\text{Ni}_{0.3}\text{Co}_{0.7}\text{O}_3$ Perovskite
Appl. Catal. A: Gen, **213**, pp.113-121.
- 18 **Lucio, F. and Rossetti, I. (2002)**
Catalytic Combustion of Hydrocarbons over Perovskites
Appl. Catal B: Environ. **38**, pp.29-37.
- 19 **Mizuno, N., Fusiwar, A. Y. and Misono, M. (1988)**
J. Chem. Soc. Chem. Commun, **61**, pp.316-318.
- 20 **Nakamura, T., Misono, M. and Nippon, K. K. (1980)**
J. Mat. Sci, **42**, pp.1679-1684
- 21 **Oliva,C., Cappelli, S., Kryukov, A., Vishniakov, A.V. and Forni, L.(2006)**
Effect of preparation parameters on the properties of $\text{La}_{0.9}\text{Ce}_{0.1}\text{CoO}_3$ catalysts: An EMR investigation,
J. Mol. Catal. A: Chem, **255**, pp.36-40

- 22 **Seiyama, T., Yamazoe, Noboru. and Eguchi.(1985)**
Characterization and activity of some Mixed metal Oxide catalysts.
Ind. Engg. Chem. Prod. Res. Dev., **24**, pp.19-27
- 23 **Simonot, Laure, Grain, Francios and Maire, Gilbert.(1997)**
A comparative study of LaCoO_3 , Co_3O_4 and $\text{LaCoO}_3\text{-Co}_3\text{O}_4$ I. Preparation,
Characterization and catalytic properties for the oxidation of CO.
Appl. Catal.B: Environ, **11**, pp.167-179.
- 24 **Sharma. A. K. (1998)**
Ph.D Thesis, Vehicular Emission Control: Studies on Non-Nobel Metal Based
Catalysts for CO and Propylene Oxidation, IIT Roorkee, August.
- 25 **Song, K. S., Hao, X. C., Sang, D. K. and Sung. K. K.(1999),**
Catalytic Combustion of CH_4 and CO on $\text{La}_{1-x}\text{M}_x\text{MnO}_3$,
Catal. Today, **47**, pp.155-160.
- 26 **Tabata, K., Matsumoto, I. and Kohiki, S. (1987)**
J. Mat. Sci, **22**, pp.2004-2007.
- 27 **Teraoka, Y. and Yamazoe, N. (1988)**
Chem. Lett, **31**, pp.389-392.
- 28 **Tanaka, H., Noritaka, M. and Makoto, M.(2003)**
Catalytic Activity and Structural Stability of $\text{La}_{0.9}\text{Ce}_{0.1}\text{Co}_{1-x}\text{Fe}_x\text{O}_3$ Perovskite
Catalysts for Automotive Exhaust Emission Control,
Appl. Catal. A: Gen., **244**, pp.371-382.
- 29 **Uenishi, M., Tanaka, H., Taniguchi, M., Tan, I. and Yokata. K.(2005)**
The reducing capability of palladium segregated from perovskite-type LaFePdO_x
automotive catalysts, Appl. Catal. A: Gen, **296**, pp.114-119.

- 30 Voorhoeve, R. J. H. and Remeika, J.P.(1972)**
Rare Earth oxides of Manganese and Cobalt riel Platinum for the Treatment of Carbon Monoxide in Auto Exhaust,
Science, 177, pp.353
- 31 Voorhoeve, R. J. H., Johnson, D. W. J. and Gallagher. K.(1977)**
Perovskite oxides: Materials Science in Catalysis,
Science, 195(4281), pp.827-832.
- 32 Wan, Li. and Qing, H. (1987)**
Improving the SO₂ resistance of perovskite –type oxidation catalyst in catalysis and automotive pollution Control, studies in surface science and catalysis,
Elsevier, Amsterdam. 30, pp.405-415.
- 33 Yao, H.C., and Yu.(1975)**
The Oxidation of hydrocarbons and CO over Metal oxides,
J. Catalysis, 36, pp.266-275.
- 34 Yamazoe, N. and Teraoka, Y.(1990)**
Catal. Today, 8, pp.175-199
- 35 Yang, X., Laitao, L. and Hua, Z.(2004),**
Structure of La_{2-x}Sr_xCoO_{4+δ}(x=0.0-1.0) and their catalytic properties in the oxidation of CO and C₃H₈
Appl. Catal. A: Gen., 272, pp. 299-303.
- 36 Yang, X., Laitao, L. and Hua, Z.(2005)**
Preparation of LaSrCoO₄ mixed oxides and their catalytic properties in the oxidation of CO and C₃H₈,
Catal. Commun. 6, pp.13-17.

- 37 **Zhang, H., Teraoka, Y. and Mamazue, N. (1987)**
Preparation of perovskite Type oxides with Large Surface area by citrate process,
Chem. Letters, pp.665-668
- 38 **Zhang, S.Y., Beckers, J. and Blik, A.(2002),**
Surface properties and catalytic performance in CO oxidation of cerium
substituted lanthanum-manganese oxides,
Appl. Catal. A: Gen., **235**, 79-92.